Preprints.org

Article

Not peer-reviewed version

Novel 5-aryl-[1,2,4]triazoloquinazoline Fluorophores: Synthesis, Comparative Studies of the Optical Properties and ICT-Based Sensing Application

Alexandra E. Kopotilova , Julia V. Permyakova , Ekaterina S. Starnovskaya , Tatyana N. Moshkina , Alexander S. Novikov , Pavel A. Slepukhin , Emiliya V. Nosova *

Posted Date: 22 October 2025

doi: 10.20944/preprints202510.1579.v1

Keywords: nitrogen heterocycles; luminescence; push-pull quinazolines; two-photon absorption; electronic-structure calculations

Preprints.org is a free multidisciplinary platform providing preprint service that is dedicated to making early versions of research outputs permanently available and citable. Preprints posted at Preprints.org appear in Web of Science, Crossref, Google Scholar, Scilit, Europe PMC.

Copyright: This open access article is published under a Creative Commons CC BY 4.0 license, which permit the free download, distribution, and reuse, provided that the author and preprint are cited in any reuse.

Preprints.org (www.preprints.org) | NOT PEER-REVIEWED | Posted: 22 October 2025 doi:10.20944/preprints202510.1579.v1

Disclaimer/Publisher's Note: The statements, opinions, and data contained in all publications are solely those of the individual author(s) and contributor(s) and not of MDPI and/or the editor(s). MDPI and/or the editor(s) disclaim responsibility for any injury to people or property resulting from any ideas, methods, instructions, or products referred to in the content.

Article

Novel 5-aryl-[1,2,4]triazoloquinazoline Fluorophores: Synthesis, Comparative Studies of the Optical Properties and ICT-Based Sensing Application

Alexandra E. Kopotilova [1], Julia V. Permyakova [1], Ekaterina S. Starnovskaya [1], Tatyana N. Moshkina [1], Alexander S. Novikov [2,3], Pavel A. Slepukhin [1,4] and Emiliya V. Nosova [1,4,*]

[1] Organic and Biomolecular Chemistry Department, Chemical Technology Institute, Ural Federal University, Mira St. 19, 620002 Ekaterinburg, Russia

[2] Institute of Chemistry, Saint Petersburg State University, 7/9 Universitetskaya Nab., 199034 Saint Petersburg, Russia

[3] Research Institute of Chemistry, Peoples' Friendship University of Russia (RUDN University), 6 Miklukho-Maklaya St., 117198 Moscow, Russia

[4] Postovsky Institute of Organic Synthesis, Ural Branch of the Russian Academy of Sciences, S. Kovalevskaya Str., 22, 620108 Ekaterinburg, Russia

* Correspondence: emilia.nosova@yandex.ru

Abstract

A synthetic approach to novel tricyclic fluorophores has been developed using 2-aryl-[1,2,4]triazolo[1,5-*c*]quinazoline-5(6*H*)-ones as key precursors. Additionally, π-extended analogues were obtained via Suzuki–Miyaura cross-coupling of 5-(4-bromophenyl)-[1,2,4]triazoloquinazoline with arylboronic acids. All compounds were fully characterized. The structure of target fluorophores was further confirmed by X-ray single crystal diffraction. Photophysical investigations revealed bright blue fluorescence in toluene (Φ_F > 95%) for all 5-aminoaryl-substituted [1,2,4]triazolo[1,5-*c*]quinazoline derivatives. Incorporation of a 9,9'-spirobisfluorene moiety led to blue-shifted absorption and emission, as well as significant reduced quantum yield. Introduction of a 1,4-phenylene spacer had little effect on the absorption, but caused a notable bathochromic shift in the emission – up to 56 nm in toluene and 142 nm in acetonitrile. [4,3-*c*]-Annelated analogue showed hypsochromic absorption shifts and moderate quantum yield (Φ_F < 34%) with unusual solvent-dependent quenching. Selected compounds exhibited pronounced solvatochromism, with emission maxima shifting by over 100 nm between non-polar and polar solvents. Furthermore, distinct acid-induced fluorescence changes were observed upon protonation, for selected compounds, indicating potential applicability as dual-mode (polarity and pH) molecular sensors. Density functional theory (DFT) calculations supported the experimental findings, revealing intramolecular charge transfer (ICT) characteristics for selected molecules.

Keywords: nitrogen heterocycles; luminescence; push-pull quinazolines; two-photon absorption; electronic-structure calculations

1. Introduction

[1,2,4]Triazoloquinazolines provide a promising molecular platform for various pharmaceutical applications [1,2] and materials sciences [3]. Pyrazoloquinazoline- and triazoloquinazoline-based organic compounds for light-emitting devices (**A–C**, Figure 1) were developed in the past decade [4,5].

The quinazolinyl moiety represents strong electron-withdrawing part of push-pull chromophores coursing considerable intramolecular charge transfer (ICT) [6]. Notably, that

© 2025 by the author(s). Distributed under a Creative Commons CC BY license.

Preprints.org (www.preprints.org) | NOT PEER-REVIEWED | Posted: 22 October 2025 doi:10.20944/preprints202510.1579.v1

annelation of the triazole cycle can be applied as important tool to enhance the electron-acceptor character of the quinazoline core, for this purpose we recently designed push-pull molecules based on [1,2,4]triazolo[4,3-*c*]quinazolines **D** (Figure 1) [7] and demonstrated that photophysical properties are influenced by the nature of arylamino residue, 3-aryltriazole fragment, as well as solvent polarity. We reported that the twisted structure of fluorophores, revealed by X-ray analysis, can inhibit strong intermolecular π–π stacking interactions thus favouring the strong solid-state emission and active aggregate form [7]. Synthetic approach to fluorophores **D** included the formation of hydrazones from 2-(4-bromophenyl)-4-hydrazinoquinazoline and arylaldehyde, oxidative cyclization of the corresponding hydrazones with bromine in glacial acetic acid at room temperature [8] and subsequent cross-coupling reaction [7]. Later we developed a synthetic approach to 5-(4-bromophenyl)-[1,2,4]triazolo[4,3-*c*]quinazolines **E** and their [1,5-*c*]-isomers **F**; we reported that the treatment of 2-(4-bromophenyl)-4-hydrazinoquinazoline with ortho esters in solvent-free conditions or in absolute ethanol leads to the formation of [4,3-*c*]-annelated triazoloquinazolines, whereas [1,5-*c*] isomers were formed in acidic media as a result of Dimroth rearrangement [9]. The bromophenyl derivatives were functionalized by introducing aminoaryl donor fragments via palladium-catalyzed cross-coupling reactions with boronic acids or their esters; the photophysical properties of two series of 5-(4′-aminophenyl-[1,1′]-biphenyl-4-yl)[1,2,4]-triazolo-quinazoline fluorophores E and F (Figure 1) were studied. The quantum yields of triazoloquinazolines with [1,5-*c*] annelation type were found to be higher than those of their [1,2,4]triazolo[4,3-*c*]quinazoline counterparts [9].

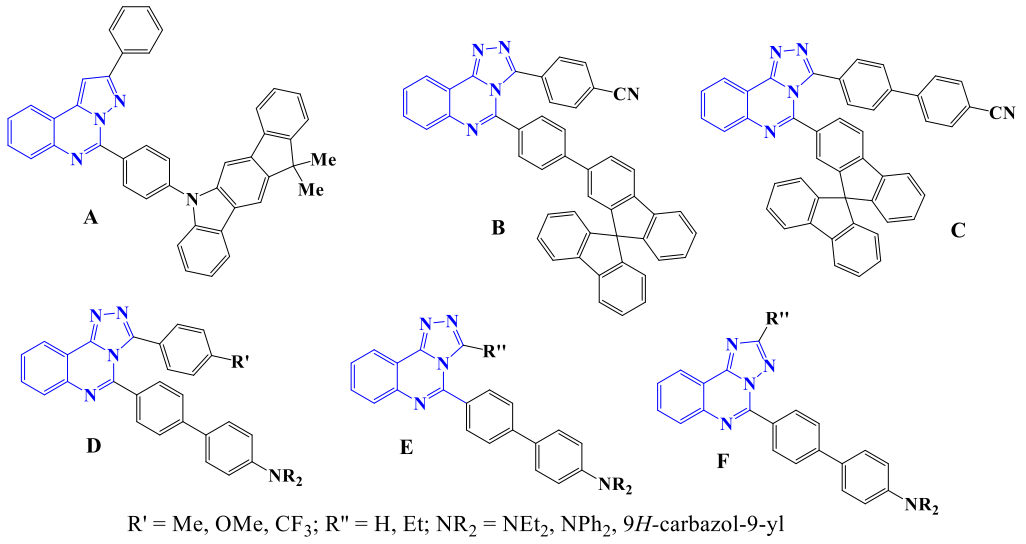

R' = Me, OMe, CF_3; R" = H, Et; NR_2 = NEt_2, NPh_2, 9*H*-carbazol-9-yl

Figure 1. Representatives of tricyclic quinazoline-based fluorophores.

Synthetic ways to 2-aryl-[1,2,4]triazolo[1,5-*c*]quinazolines are limited. The formation of [1,5-*c*] isomer of triazoloquinazoline from arylhydrazone in the presence of $PhI(OAc)_2$ at 50 °C was mentioned [10], however, the evidence of structure and Dimroth rearrangement details were not discussed. Some derivatives were obtained by the condensation of anilino-substituted bromotriazole with 1,1-carbonyldiimidazole and subsequent incorporation of aryl fragment by cross-coupling reaction [11]. The synthesis of 2,5-diphenyl-[1,2,4]triazolo[1,5-*c*]quinazoline was achieved through the condensation of 4-iminoquinazoline-3-amine with benzoyl chloride [12]. Anthranylhydrazide, arylamidine and cyanamide were used as reagents for the synthesis of 2-aryl-5-amino[1,2,4]triazolo[1,5-*c*]quinazolines [13]. The formation of limited range of 2,5-diaryl-[1,2,4]triazolo[1,5-*c*]quinazolines was achieved by the reaction of 2-aryl-3-aminoquinazolin-4-one, benzoyl chloride and ammonium acetate [14].

An approach to 2-aryl-[1,2,4]triazolo[1,5-*c*]quinazolin-5-one based on the interaction of anthranilonitrile, methyl chloroformate as one-carbon synthon and arylcarbohydrazide, opens wide opportunities for varying the substituent in position 2 [15]. Diverse modifications of position 5 by nucleophilic substitution of chlorine were performed, some S_N reactions afforded valuable biologically active compounds [16]; however, incorporation of aryl fragment into position 5 by cross-

© 2025 by the author(s). Distributed under a Creative Commons CC BY license.

Preprints.org (www.preprints.org) | NOT PEER-REVIEWED | Posted: 22 October 2025 doi:10.20944/preprints202510.1579.v1

coupling reactions in 2-aryl-5-chloro-[1,2,4]triazolo[1,5-*c*]quinazolines has not been investigated to date.

Herein, we present a concise two-step approach to novel tricyclic fluorophores derived from 2-aryl-[1,2,4]triazolo[1,5-*c*]quinazolin-5(6*H*)-ones. Furthermore, π-extended analogues were accessed via functionalization of 5-(4-bromophenyl)-[1,2,4]triazoloquinazoline. All compounds were comprehensively characterized by analytical and spectroscopic techniques, including single-crystal X-ray diffraction. Their photophysical properties were evaluated by spectrofluorimetric methods, and structure-property relationships were explored with respect to conjugation length, annelation type, and electronic effects of substituents. Solvatochromic behaviour and acid-responsive properties were investigated for a series of [1,2,4]triazoloquinazolines, demonstrating their potential as polarity-sensitive and pH-responsive molecular sensors. Complementary DFT calculations were performed to gain insight into the electronic structure and were correlated with the experimental photophysical data.

2. Results

2.1. Synthesis

A synthetic strategy toward 2,5-diaryl-[1,2,4]triazolo[1,5-*c*]quinazolines **6a-j** is depicted in Scheme 1. *N*-(2-Cyanophenyl)carbamate **2**, prepared from 2-aminobenzonitrile **1** and ethyl chloroformate, reacted with the corresponding arylhydrazide **3a-c** to give key intermediates 2-aryl-[1,2,4]triazolo[1,5-*c*]quinazolin-5-ones **4a-c.** This process involves a tandem reaction: nucleophilic addition of an arylhydrazide **3** to the nitrile group of intermediate **2**, followed by cyclocondensation, as described in [17]. Prolonged reflux of quinazolinone **4a-c** in phosphorus oxychloride in the presence of N,N-diisopropylethylamine (DIPEA) afforded the corresponding 5-chloro derivatives **5a-c** [17]. Subsequent Suzuki-Miyaura cross-coupling reactions with arylboronic acids or their esters furnished the target products **6a-j** in unoptimized yields ranging from 20 to 70%.

© 2025 by the author(s). Distributed under a Creative Commons CC BY license.

Preprints.org (www.preprints.org) | NOT PEER-REVIEWED | Posted: 22 October 2025 doi:10.20944/preprints202510.1579.v1

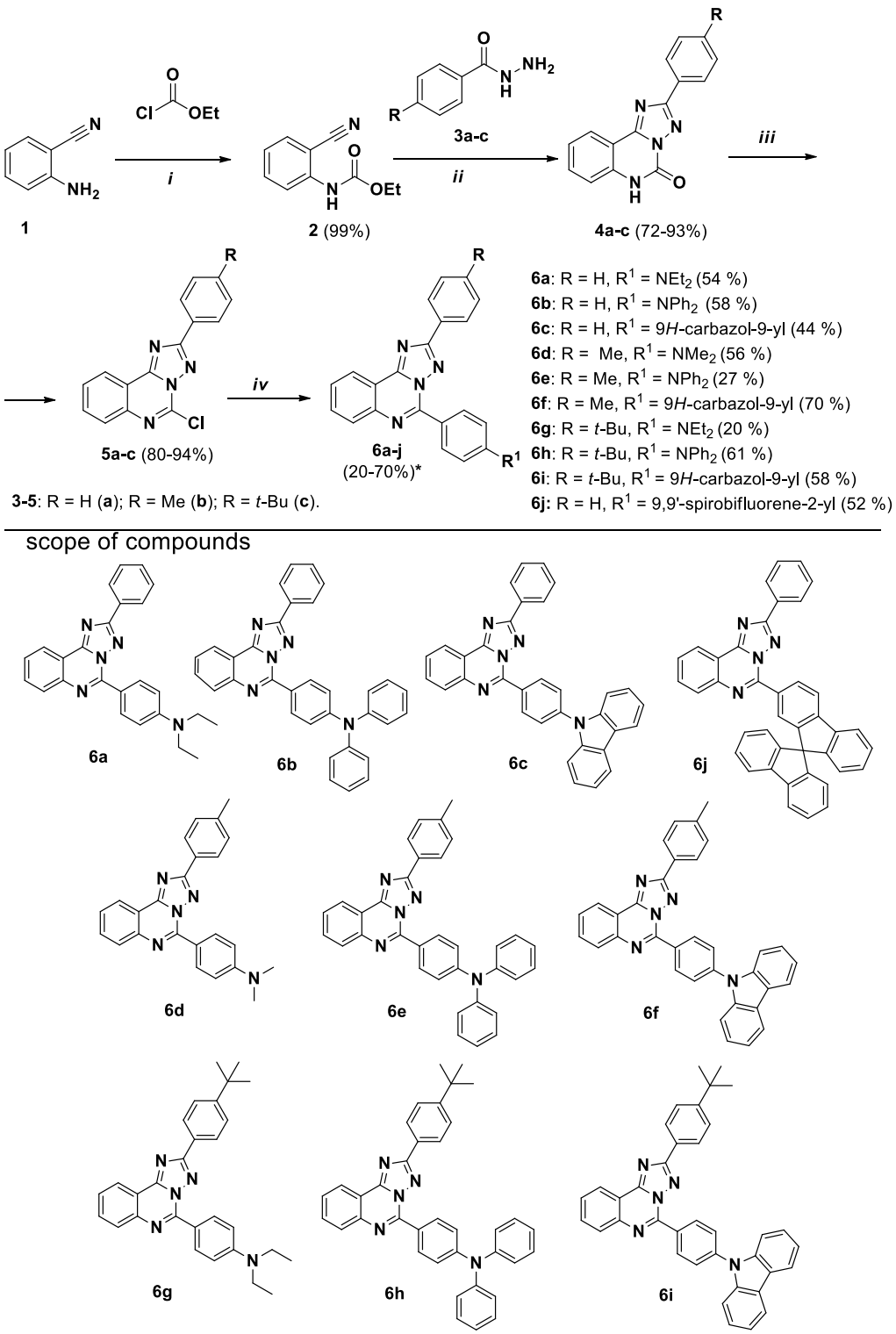

Scheme 1. Synthesis of quinazolines **6a-j**. *Reagents and conditions*: ***i***) K_2CO_3, THF, 85 °C, 24 h; ***ii***) DMF, 120 °C, 12 h; ***iii***) $POCl_3$, DIPEA, 110 °C, 20 h; ***iv***) corresponding arylboronic acid or ester, $PdCl_2(PPh_3)_2$, PPh_3, K_2CO_3, toluene, EtOH, H_2O, argon, 85 °C, 14–30 h. *unoptimized yields.

Additionally, we synthesized 2-phenyl[1,2,4]triazolo[1,5-*c*]quinazoline **10** (Scheme 2), featuring an extended π-conjugation system, and its [4,3-*c*]-annelated counterpart **11** (Scheme 2), to investigate the effect of conjugation length and annulation type on the photophysical properties of the [1,2,4]triazoloquinazoline series. It was demonstrated that the intermediate **8a** could be formed by refluxing 4-hydrazinoquinazoline **7,** prepared as described previously [8], with triethoxymethylbenzene in acetic acid for 16 h (Scheme 2). In contrast, the [4,3-*c*]-annulated counterpart isomer **9** was obtained in good yield from the same reagents upon refluxing under neat

© 2025 by the author(s). Distributed under a Creative Commons CC BY license.

Preprints.org (www.preprints.org) | NOT PEER-REVIEWED | Posted: 22 October 2025 doi:10.20944/preprints202510.1579.v1

conditions or in absolute ethanol. In this case the setup included a drying tube filled with calcium chloride to protect the reaction from atmospheric moisture. Notably, transformation of compound **8a** into its [1,5-*c*] isomer **9** was observed upon prolonged heating under acidic conditions via a Dimroth rearrangement [9].

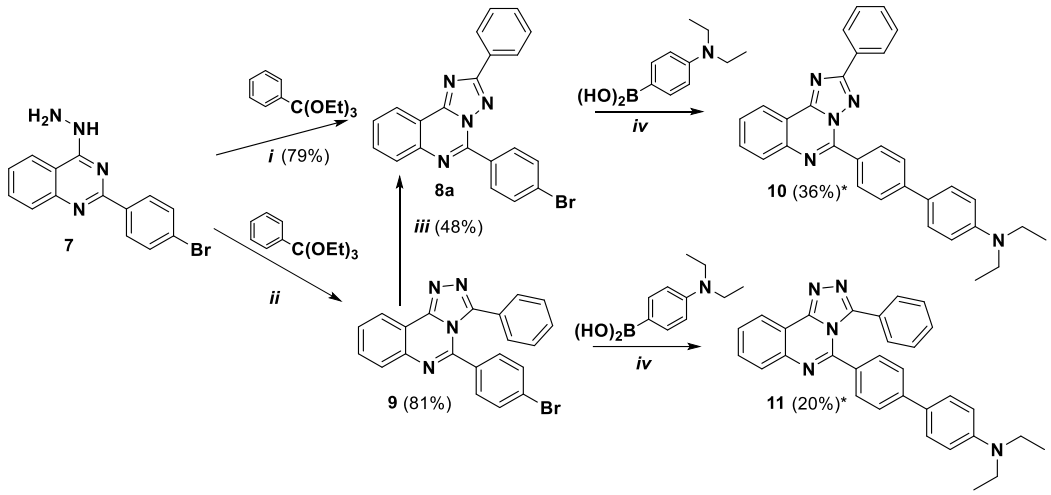

Scheme 2. Synthesis of 2-phenyl[1,2,4]triazolo[1,5-*c*]quinazoline **10** and 3-phenyl[1,2,4]triazolo[4,3-*c*]quinazoline **11.** *Reagents and conditions*: ***i)*** CH_3COOH, reflux, 16 h; ***ii***) reflux, 16 h; ***iii***) CH_3COOH, reflux, 20 h; ***iv***) $PdCl_2(PPh_3)_2$, PPh_3, K_2CO_3, toluene, EtOH, H_2O, argon, 85 °C, 11–16 h. *unoptimized yields.

Finally, 9,9'-spirobifluorene-contained 2-phenyl- and 2-ethyl-[1,2,4]triazolo[1,5-*c*]quinazolines **12a** and **12b** were obtained from the corresponding bromo derivatives **8a,b** [9], Scheme 3.

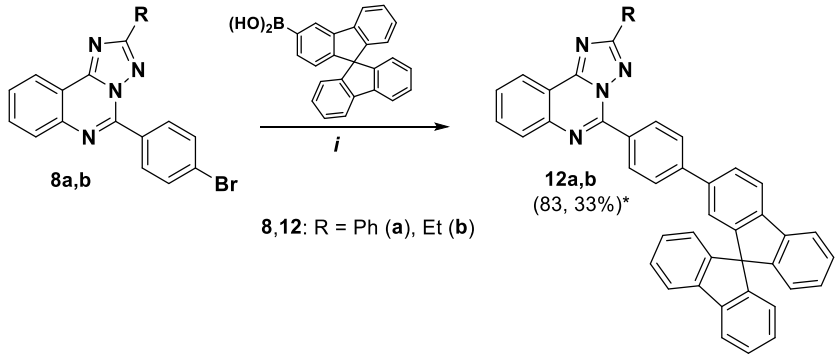

Scheme 3. Synthesis of 9,9'-spirobifluorene-substituted [1,2,4]triazolo[1,5-*c*]quinazolines **12a,b**. *Reagents and conditions*: ***i)*** $PdCl_2(PPh_3)_2$, PPh_3, K_2CO_3, toluene, EtOH, H_2O, argon, 85 °C, 14 h. *unoptimized yields.

The structures of the intermediate compounds were confirmed by ^1H NMR spectroscopy and electron ionization mass spectrometry (EI-MS), Figures S1–S10. For the target compounds, full characterization was performed using ^1H and ^{13}C NMR spectroscopy, EI-MS, and elemental analysis data, Figures S12–S25. Additionally, a ^1H–^1H NOESY experiment was carried out for one representative compound to assist in the assignment of NMR signals to specific hydrogen atoms (Figure S17 (b)).

According to X-ray diffraction analyses, Figure 2, Tables S1–S8, performed on single crystals of compounds **6f**, **6g**, **10** and **12a**, the molecular structures showed the expected connectivity and spatial arrangement.

According XRD data, the compound **6f** is crystallized in the centrosymmetrical space group as solvate with $CHCl_3$ (1:1). The molecule of $CHCl_3$ is disordered into two positions and forms the shortened C-H…N contacts with the nitrogen's atoms of the heterocycle. The geometry of the heterocyclic compound (the bond distances and angles) is near to the expectation. The heterocyclic core of the molecule is planar, the plane of the phenylene bridge in the molecule is turned toward

© 2025 by the author(s). Distributed under a Creative Commons CC BY license.

Preprints.org (www.preprints.org) | NOT PEER-REVIEWED | Posted: 22 October 2025 doi:10.20944/preprints202510.1579.v1

plane of the heterocycle on the angle 40°, the plane of the carbazole's moiety is oriented approximately in the plane of the tricyclical system. The molecular crystal packing is layered. The layers is oriented in the plane (1 0 0). The distances between the molecular layers 3.45-3.50 Å and significantly shortened π-π-contacts (lesser when 3.35 Å) between molecules are not observed.

The compound **6g** crystallizes in a centrosymmetric space group of the triclinic system. The bond lengths and angles in the molecule are close to the expected values. The heterotricyclic core is planar within 0.04 Å. The *t*-Bu-C_6H_4 group is approximately coplanar with the heterocycle. The diethylaminophenylene group exhibits disorder of the Et and C_6H_4 substituents over two positions, with significant dihedral angles (30° and 40°) between the C_6H_4 moiety and the heterocycle (Fig. 2). The C_{sp^2}–N and C_{sp^3}–N interatomic distances for the N(2) atom are well resolved. The shortened intermolecular contacts in the crystal primarily involve the disordered moieties, making precise evaluation of their geometry challenging.

The compound **10** crystallizes in a centrosymmetric space group of the monoclinic system. The heterocyclic moiety is planar, and the phenyl substituent is approximately coplanar with the heterocycle. The N atom of the diethylamine group has a planar environment and shows strong conjugation with the C_6H_4 moiety (C_{sp^2}–N distance 1.39 Å). In the crystal, shortened centrosymmetric intermolecular π–π contacts are observed between neighboring heterocycles.

The compound **12a** crystallizes in a centrosymmetric space group of the triclinic system, with two $CHCl_3$ molecules in the lattice. The heterocyclic moiety is planar; the phenyl substituent is approximately coplanar with the heterocycle (dihedral angle 16°), while the C_6H_4 substituent is rotated toward the plane of the heterocycle by 28°. In the crystal, shortened centrosymmetric intermolecular π–π contacts are observed between adjacent heterocycles, with interatomic distances of 3.4 Å.

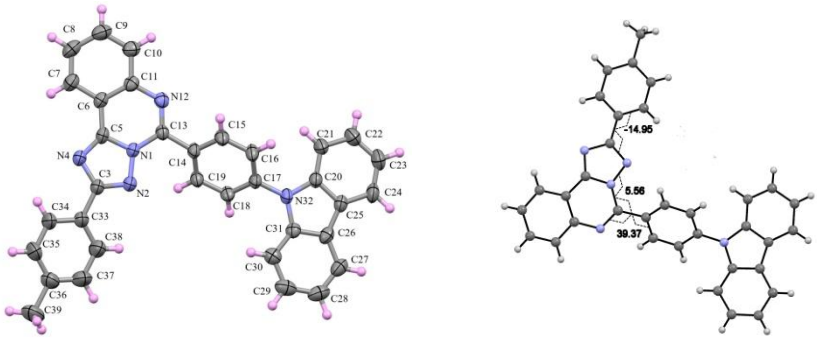

Compound **6f**

(**a**) (**b**)

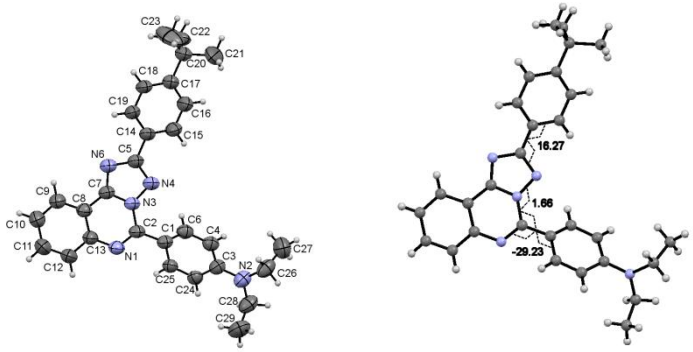

Compound **6g**

(**a**) (**b**)

© 2025 by the author(s). Distributed under a Creative Commons CC BY license.

Preprints.org (www.preprints.org) | NOT PEER-REVIEWED | Posted: 22 October 2025 doi:10.20944/preprints202510.1579.v1

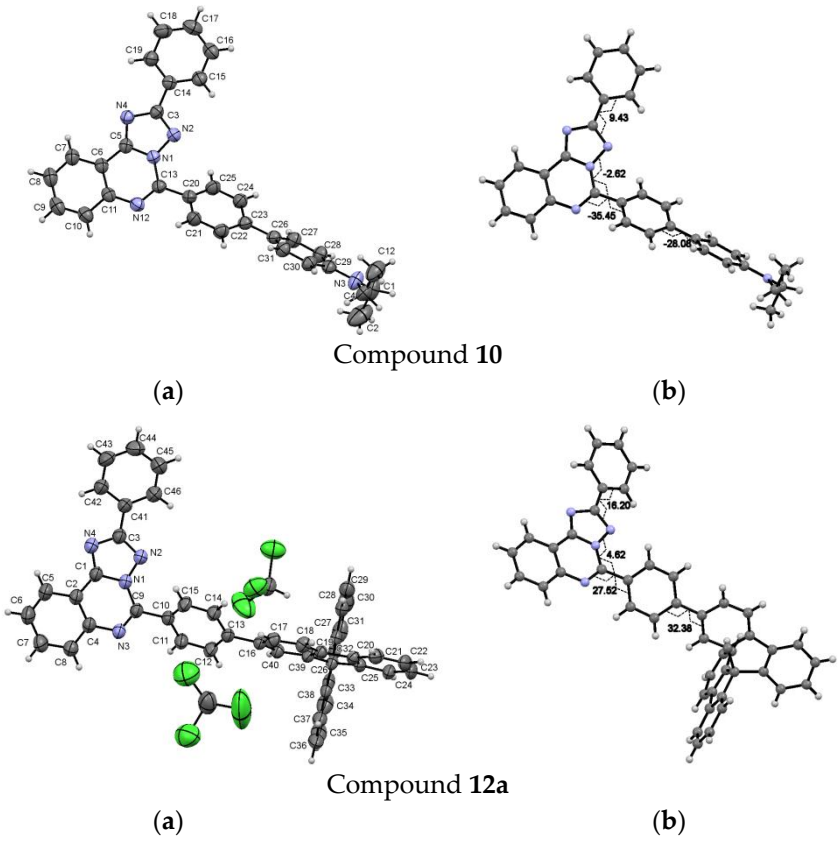

Figure 2. (a) Molecular structure of compounds **6f, 6g**, **10** and **12a** in the thermal ellipsoids of 50% probability); (b) Selected torsion angles of compounds **6f, 6g**, **10** and **12a.**

2.2. UV-Vis and Fluorescence Spectroscopy

The photophysical properties of the synthesized quinazolines **6a-j, 10, 11** and **12a,b** were investigated in two solvents of different polarity, toluene (ε_r = 2.39 [12]), and acetonitrile (MeCN) (ε_r = 36.64 [12]), at room temperature (see SI, Figure S26) and the corresponding data are summarized in Table 1.

Table 1. Photophysical properties of fluorophores **6a-k, 10, 11** and **12a,b**, in solution (c = 10^{-5} M) and solid state at r.t.

Comp.	Solvent/ solid state	λ_{abs}, nm, ε (10^4 $M^{-1}cm^{-1}$)	λ_{em} [b], nm	$\Delta\nu_{st}$ [c], cm^{-1}	Φ_F [d], %
6a	Toluene	376 (2.64)	425	3070	>95
	MeCN	284 (2.35), 376 (3.53)	459	4810	>95
	Solid	-	511	-	*
6b	Toluene	383 (1.92)	459	4320	81
	MeCN	252 (4.21), 285 (2.30), 375 (2.61)	544	8280	51
	Solid	-	456	-	45
6c	Toluene	342 (1.47), 355 (1.48)	423	4530	>95
	MeCN[a]	254, 277 sh, 340	507	9690	87
	Solid	-	459, 481(sh)	-	20
6d	Toluene	369 (1.96)	421	3350	>95
	MeCN	253 (4.18), 284 (2.56), 367 (2.69)	457	5370	>95
	Solid	-*	433	-	*
6e	Toluene	289 (3.35), 382 (2.49)	459	4390	91
	MeCN	259 (1.23), 284 (0.87), 375 (0.73)	539	8110	52
	Solid	-	492	-	38
6f	Toluene	342 (0.95), 355 (0.92)	421	4420	>95

© 2025 by the author(s). Distributed under a Creative Commons CC BY license.

Preprints.org (www.preprints.org) | NOT PEER-REVIEWED | Posted: 22 October 2025 doi:10.20944/preprints202510.1579.v1

	MeCN[a]	259, 278 sh, 340	506	9650	88
	Solid	-	434	-	28
6g	Toluene	376 (2.88)	425	3070	>95
	MeCN	254 (4.39), 286 (2.48), 376 (3.19)	460	4860	>95
	Solid	-	448, 474	-	*
6h	Toluene	292 (1.23), 381 (1.43)	457	4370	>95
	MeCN	259 (1.43), 284 (1.03) sh, 375 (0.77)	540	8150	53
	Solid	-	463	-	37
6i	Toluene	342 (0.92), 355 (0.89)	420	4360	>95
	MeCN[a]	284, 278 sh, 340	506	9650	84
	Solid	-	432	-	*
6j	Toluene	296 (2.48), 309 (2.73), 339 (2.58)	376, 396, 417 sh	4250[e]	7
	MeCN	252 (1.90), 270 (1.48), 307 (1.09), 330 (1.0)	400	5300	4
	Solid		403, 422	-	*
10	Toluene	384 (1.88)	481	5250	>95
	MeCN	222 (0.53), 262 (1.71), 377 (0.83)	601	9890	35
	Solid	-	513	-	6
11	Toluene	363 (1.21)	493	8324	17
	MeCN	271 (7.34), 356 (1.46)	616	11860	34
	Solid	-	492	-	*
12a	Toluene	284(9,08), 309(6,00)	398, 416, 440 sh	8324	19
	MeCN	296 (1,54), 308(1,87), 335(2,26)	442	7226	77
	Solid	-	431, 449, 482 sh	-	*
12b	Toluene	309 (2.87), 337 (3.04)	392, 412, 437 sh	5402[e]	60
	MeCN[a]	308, 331	433	7120	>95
	Solid	-	417, 439, 469 sh	-	*

[a] Poor soluble. [b] Excitation at the lowest energy absorption peak. [c] Stokes shift was calculated relative to the lowest energy absorption peak and rounded to tens. [d] Absolute fluorescence quantum yield was measured according to a reported procedure [18] using Horiba-Fluoromax-4 spectrofluorometer equipped with integrating sphere. [e]Relative to middle peak of emission. * Data was not measured.

5-Aminoaryl-substituted series of [1,2,4]triazolo[1,5-*c*]quinazolines **6a-i** (Table 1) exhibit long-wavelength absorption bands in the range of 325–425 nm and emission maxima between 420 and 459 nm in toluene. It was found that solvent polarity has little effect on the absorption spectra; however, a pronounced bathochromic shift of the emission maximum is observed upon going from toluene to acetonitrile (Figure 3). This solvent-dependent emission shift is significant for (diphenylamino)phenyl and (carbazolyl)phenyl derivatives **6b,c,e,f,h,i**. These findings indicate an increase in the molecular dipole moment upon photoexcitation, likely resulting from electron density redistribution and dipole formation.

© 2025 by the author(s). Distributed under a Creative Commons CC BY license.

Preprints.org (www.preprints.org) | NOT PEER-REVIEWED | Posted: 22 October 2025 doi:10.20944/preprints202510.1579.v1

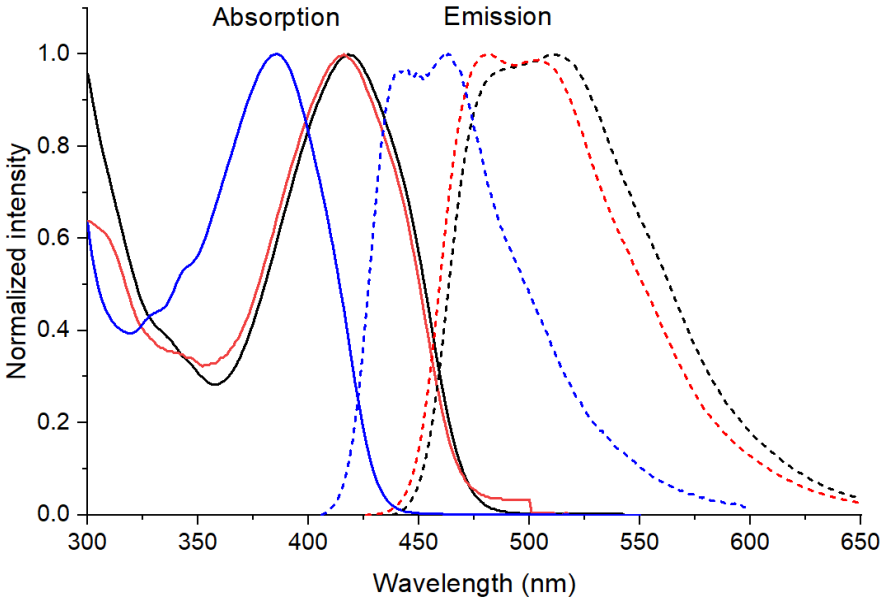

Figure 3. Normalized absorption (dotted line) spectra in MeCN and emission spectra in toluene (dashed line) and acetonitrile (solid line) of compounds **6a** (black line), **6b** (red line) and **6c** (blue line).

Notably, the nature of the aryl substituent at the triazole ring of considered compounds **6a-i** has little influence on the spectrofluorimetric properties. In contrast, the electronic character of the aryl donor fragment at position 5 of [1,2,4]triazolo[1,5-*c*]quinazoline core significantly affects the photophysical behaviour. For instance, the absorption maxima of carbazolyl-substituted derivatives **6c**, **6f**, and **6i** are hypsochromically shifted by approximately 30–40 nm relative to their Et_2N- and Ph_2N-substituted counterparts, Figure 3, Table 1. The emission colour turns from blue to yellow upon changing the electron donor fragment from diethylamino- to carbazolyl- and further to diphenylamino- group in acetonitrile (Figure 4(a)).

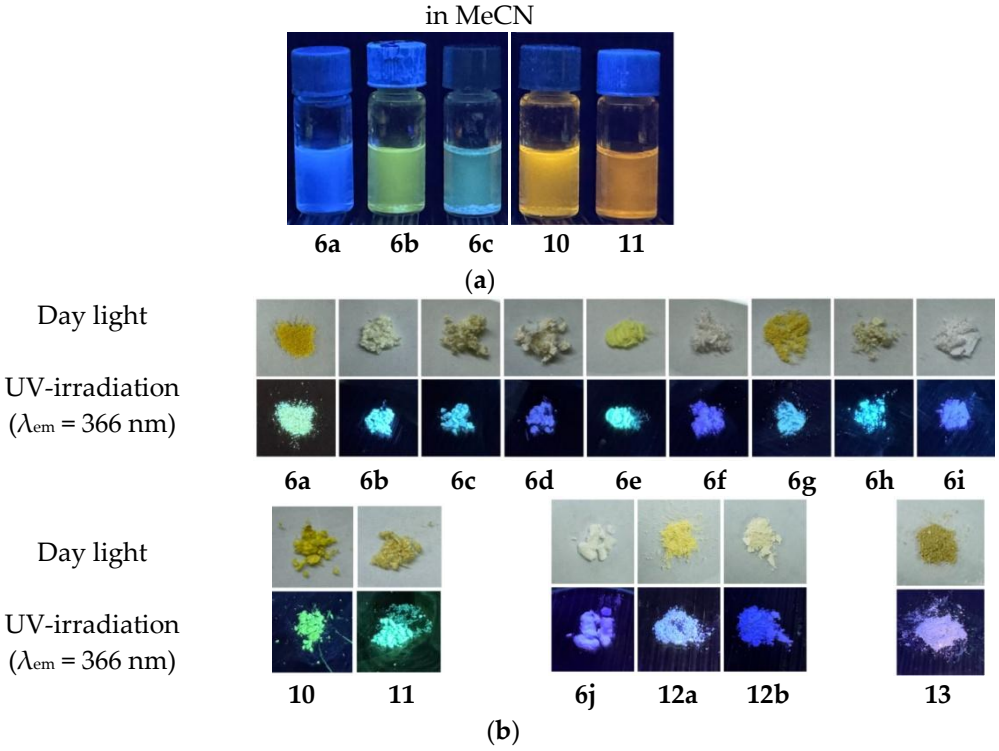

© 2025 by the author(s). Distributed under a Creative Commons CC BY license.

Preprints.org (www.preprints.org) | NOT PEER-REVIEWED | Posted: 22 October 2025 doi:10.20944/preprints202510.1579.v1

Figure 4. (a) Photograph of solutions of the compounds **6a-c, 10** and **11** in acetonitrile under UV-irradiation (λ_{em} = 366 nm). (b) Photograph of the compounds **6a-j, 10, 11** and **12a,b** in the solid state (powder) in daylight and under UV-irradiation (λ_{em} = 366 nm).

Aminoaryl-substituted compounds **6a–i** exhibit strong blue luminescence (Table 1) with fluorescence quantum yields (Φ_F) exceeding 95% in toluene and above 52% in acetonitrile. Remarkably, their luminescent properties are retained in the solid (powder) state (Figure 4(b)). It was shown that the presence of 9,9′-spirobisfluorene residue at position 5 of [1,2,4]triazolo[1,5-*c*]quinazoline core (compound **6j**) resulted in blue-shifted absorption and emission bands as well as significant reduction of Φ_F regardless solvent (Table 1).

The introduction of an additional 1,4-phenylene spacer (compound **10** *vs.* **6a**) has little effect on the absorption spectrum (Figure 5(a)), but induces a significant bathochromic shift in the emission band – by 56 nm in toluene, while retaining a high fluorescence quantum yield (>95%), and by 142 nm in acetonitrile, where the quantum yield decreases to 35% (Table 1, Figure 5(b)). The presence of [4,3-*c*]-annelated fragment (compound **11** vs. **10**) leads to a hypsochromic shift of the absorption maximum, presumably due to decreased molecular planarity and, consequently, a reduction in conjugation length, caused by steric hindrance from adjacent substituents. A similar twisting tendency and corresponding spectral behaviour have been previously observed in related 3-ethyl-substituted [1,2,4]triazolo[4,3-*c*]quinazoline derivatives [9]. The fluorescence quantum yield of compound **11** does not exceed 34% in solution, and, unlike the other compounds in the series, **11** exhibits decreased emission intensity when going from acetonitrile to toluene (Table 1).

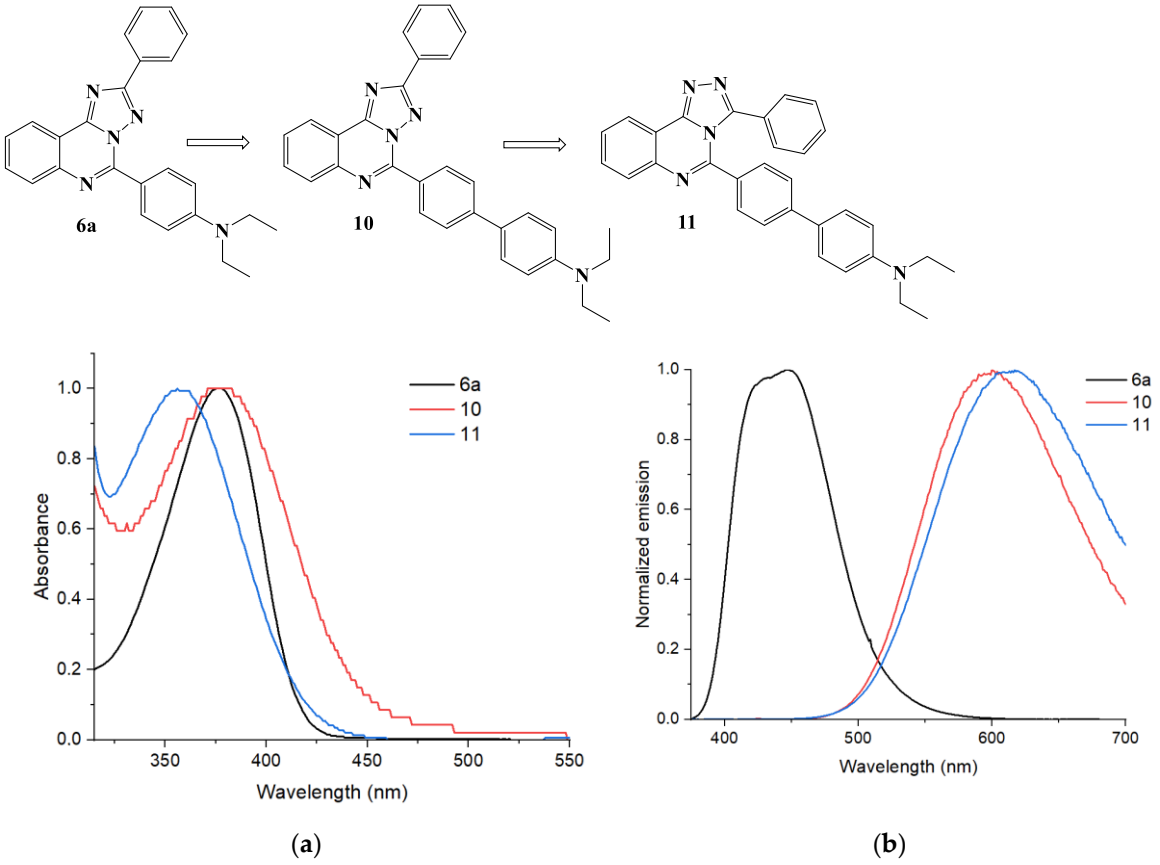

Figure 5. Combined normalized absorption (a) and emission (b) spectra of phenyl-substituted triazoloquinazolines **6a**, **10** and **11** in MeCN (C = 10^{-5} M).

Compounds **12a,b** exhibited absorption with long-wavelength maximum around 330 nm, along with red-shifted emission bands compared to their counterpart **6j**. Interestingly, that introduction of additional phenylene ring into the structure of 9,9′-spirobisfluorene-substituted derivatives (**12a,b** vs. **6j**) led to a pronounced enhancement of the emission intensity and the Et-substituted derivative **12b**

© 2025 by the author(s). Distributed under a Creative Commons CC BY license.

Preprints.org (www.preprints.org) | NOT PEER-REVIEWED | Posted: 22 October 2025 doi:10.20944/preprints202510.1579.v1

showed a remarkable Φ_F, reaching 95% in MeCN. Both compounds **12a,b** demonstrated higher Φ_F values in MeCN compared to toluene solution.

In the solid state (powder form), compounds **6a-j**, **10**, **11** and **12a,b** are emissive in the violet–green region (Figure 4(b)), with emission maxima observed in the range of 403–513 nm, Figure S27, Table 1. The absolute quantum yields in the solid state were found to reach 37%, Table 1.

2.3. Solvatochromic Effect

Solvatochromic properties of compounds **6a–c**, **10** and **11** were analyzed in a series of solvents of varying polarity, Figure S28 (cyclohexane, toluene, 1,4-dioxane, EtOAc, THF, CH_2Cl_2, DMSO, and MeCN). It was found that the emission colour of compound **6a** remains nearly unaffected by the nature of the solvent, which likely indicates negligible changes of dipole moment upon photoexitation. Other compounds **6b** and **6c** appear to be sensitive to changes in the medium, exhibiting solvatochromism with emission colour from deep blue to yellow. The most pronounced solvent-dependent behaviour was observed for compounds **10** and **11**, colour of solutions turns from blue to orange with increasing solvent polarity. Notably, together with the visible changes in solution colour, compounds **6b** and **10** exhibit intense fluorescence in all solvents, indicating their potential as solvatochromic fluorescent sensors.

Further, absorption and emission spectra were recorded for compounds **6a-c** and **10** in the same solvents. The maximum of the absorption bands were revealed to be weakly dependent on the solvent polarity (Tables S9–S11), indicating a low molecular dipole moment in the ground state.

In agreement with visual observations, compound **6a** display bright and intense blue emission in the region (380–500 nm) and shows a relatively small red-shift (Figure 6, Figure S29). In contrast, the emission maxima of triazoloquinazolines **6b** and **6c** are red-shifted to 600 nm in polar solvents. Finally, the emission of compound **10** extends over a wide spectral region from 400 to 750 nm (Figure 6, Figure S29).

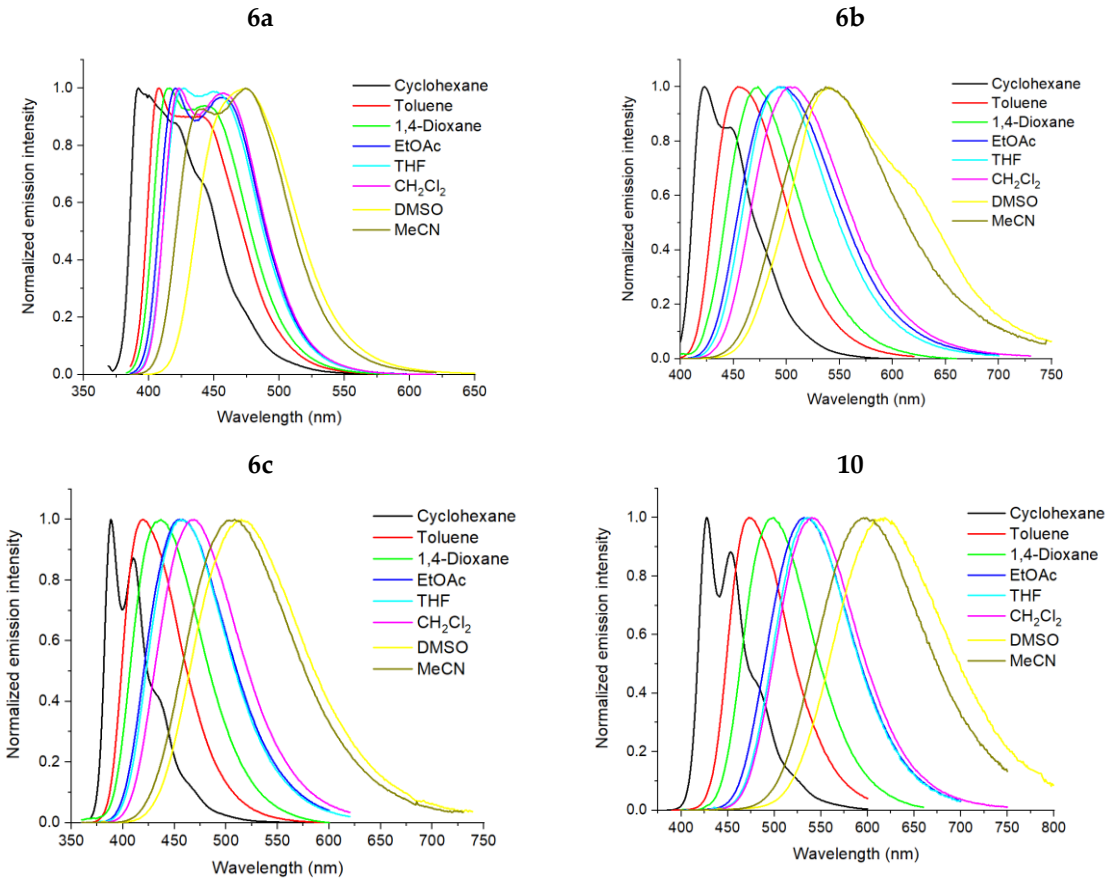

Figure 6. Combined normalized emission spectra of compounds **6a**, **6b**, **6c** and **10** in different solvents.

© 2025 by the author(s). Distributed under a Creative Commons CC BY license.

Preprints.org (www.preprints.org) | NOT PEER-REVIEWED | Posted: 22 October 2025 doi:10.20944/preprints202510.1579.v1

In nonpolar cyclohexane, the fluorescence spectra of compounds **6a–c** and **10** exhibits well-resolved, structured emission bands, indicative of a rigid, less polar excited state with limited solvent–solute interactions. In more polar solvents (except DMSO), compound **6a** displays a dual-emission profile with two distinct peaks. This effect likely arises from interplay between locally excited (LE) and intramolecular charge-transfer (ICT) states, with solvent polarity modulating their relative contributions. The similar behavior of emission spectra were observed for small D-A molecule with directly attached electron donor fragment to electron-withdrawing core.[19] The emission of other compounds **6b**, **6c** and **10** becomes featureless together with the broadened full width at half maximum (FWHM), reflecting enhanced vibronic relaxation and stronger stabilization of the excited state by solvent dipoles. This behaviour suggests that the electronic transitions involve significant charge redistribution, which is effectively stabilized in polar media. The increscent in red-shift degree of emission spectra, probably due to reinforce donor-acceptor interaction in compounds **6b**, **6c** and **10** compared to **6a.** Generally, correlations between structure and emission spectra correspond to literature

The correlations observed between the molecular structures and solvatochromic behavior of compounds **6a–c** and **10** upon increasing solvent polarity agree with literature reports on analogous systems [19] where transformation of an excited state character from the locally-excited (LE) state to the charge-transfer (CT) state is observed in the emission spectra.

Further the change in dipole moment (Δμ) between the ground and exited ICT-state was estimated from the Ravi equation [20], using the slope of the Stokes shift dependence on the empirical solvent polarity parameter (E^N_T) proposed by Reichardt [21], Tables S7–S9, Figure S29. Other methods for estimation of Δμ (Lippert-Mataga [22,23], Bakhshiev [24]) were also tested; however they yielded low correlation coefficient ($R^2 < 0.9$), indicating limited reliability for the present series of compounds.

Table 3. Solvent cavity (Onsager) radius and data from Ravi plot for quinazolines **6b**, **6c** and **10**.

Comp.	a_1, [a] A	Slope	R^2	Δμ, D
6b	5.79	9539	0.98	7.46
6c	5.78	13735	0.95	8.93
10	5.71	11343	0.97	7.97

[a] Solvent cavity radius, calculated from the Suppan's equation [25]: $a = \sqrt[3]{\frac{3M}{4N\pi\delta}}$, where with δ is the density of the solute (δ is assumed to 1.0 g/cm^3), *M is* the molecular weight of the solute, and *N* the Avogadro number.

The difference in dipole moment for all studied triazoloquinazoline derivatives was calculated to be approximately 7.5–9 D, Table 3, confirming that the excited state of all fluorophores is more polar than the ground state. This increase in polarity corresponds to the intramolecular charge transfer (ICT) character of the exited state formed upon photoexitation.

2.4. Acid-Induced Spectral changes of Fluorophores

Since the photophysical properties of heteroaromatic fluorophores containing nitrogen atoms can be affected by protonation [7,26,27] the spectral response of the selected compounds **6a** and **10** to acid was examined to assess their potential for acidochromic applications. Initially, the response of the compounds **6a** and **10** solved in toluene to excess of trifluoroacetic acid was evaluated visually under UV-light, which revealed full quenching of luminescence, Figure S31. Acid was (C = 0.01 M) then added stepwise to toluene solutions (C = 10^{-5} M) of **6a** and its biphenylene counterpart **10**, and the spectral changes were recorded to monitor the protonation process. Upon gradual addition of TFA, distinct spectral responses were observed, Figure S31, S32. In case of compound **6a**, the absorption maximum exhibited a bathochromic shift of 83 nm (Figure 7(a)), probably indicative of protonation at the electron-deficient triazoloquinazoline core, which increase intramolecular charge transfer (ICT). Conversely, compound **10** displayed a hypsochromic shift of 58 nm (Figure 7(b)), suggesting protonation of donating aminoaryl moiety and destabilization of the excited state. In both systems, steady-state fluorescence measurements revealed progressive quenching of emission intensity upon acid addition, with near-complete suppression observed at high

© 2025 by the author(s). Distributed under a Creative Commons CC BY license.

Preprints.org (www.preprints.org) | NOT PEER-REVIEWED | Posted: 22 October 2025 doi:10.20944/preprints202510.1579.v1

concentrations of acid 2000 eq and 750 eq, respectively. This quenching effect is likely associated with increased non-radiative decay pathways and disruption of π-conjugation following protonation. In both cases protonation process was reversible, and the colour of toluene solution turns to initial state after addition of TEA in acidic solutions (Figure S31).

To support the proposed protonation sites, NMR experiments were performed. Upon addition of TFA-d_1, characteristic downfield shifts were observed for the hydrogen atoms of NEt_2 group, as well as atoms in phenylene ring adjacent to NEt_2 group, Figure S34 (b). Contrary, signals of compound **6a** remain almost unchanged, Figure S34 (a).

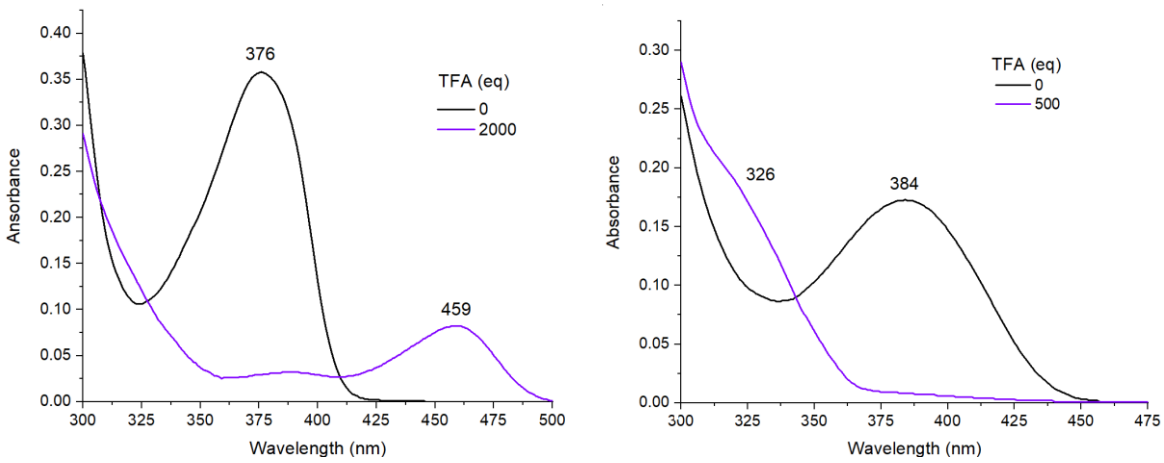

(**a**) (**b**)

Figure 7. Absorption spectra of compounds **6a** (a) and **10** (b) in pure toluene and upon addition of excess of TFA.

These findings highlight the crucial role of molecular architecture in displaying the acid-responsive optical behaviour of considered donor–acceptor fluorophores. The distinct sites of protonation observed for compounds **6a** and **10** can be rationalized by considering the degree of π-conjugation between the electron-donating and electron-accepting moieties. In compound **6a**, the diethylaminophenyl group is directly attached to the electron-deficient triazoloquinazoline core. This close π-conjugation facilitates electron withdrawal from the donor unit by the electron-deficient triazoloquinazoline core, thereby decreasing the electron density on the amino nitrogen and lowering its basicity. As a result, protonation preferentially occurs at the heterocyclic core, promoting intramolecular charge transfer (ICT) and leading to a pronounced bathochromic shift in the absorption spectrum. In contrast, compound **10** contains an additional phenylene spacer between the donor and acceptor units, effectively interrupting direct conjugation. This spatial separation weakens the electronic communication between the diethylaminophenyl donor and the heterocyclic acceptor. Consequently, the electron-rich aminoaryl group remains basic and accessible site for protonation. Protonation at this site diminishes the donor strength and destabilizes the excited state, resulting in a hypsochromic shift. Thus, the presence of the phenylene spacer in **10** not only alters the photophysical response but also shifts the protonation preference from the acceptor to the donor moiety due to reduced conjugation and charge delocalization.

2.5. Quantum-Chemical Calculations

To gain insights into the electronic features of investigated fluorophores **6**, **10**, **11** and **12**, the distributions of the frontier molecular orbitals, i.e., the highest occupied molecular orbital (HOMO) and the lowest unoccupied molecular orbital (LUMO), were simulated using density functional theory (DFT) at the B3LYP/6-31G*//PM6 level with Gaussian-09, as shown in Figure S12. The HOMO electrons in compounds **6a-d**, **6h**, **6j**, **10**, **11**, and **12a,b** are predominantly localized on the electron-donating aminoaryl or 9,9′-spirobifluorene units, including the phenylene spacer and in case of series **6** the quinazoline core (this contribution is particularly pronounced in compound **6a**). In contrast, the LUMO electron density is largely shifted toward the electron-deficient phenyl(aryl)-substituted [1,2,4]triazoloquinazoline core, indicating an intramolecular charge transfer upon excitation.

© 2025 by the author(s). Distributed under a Creative Commons CC BY license.

Preprints.org (www.preprints.org) | NOT PEER-REVIEWED | Posted: 22 October 2025 doi:10.20944/preprints202510.1579.v1

Analysis of the molecular orbital (MO) overlap shows that in the series of compounds **6**, the donor–acceptor separation is relatively weaker compared other compounds, in which ICT character becomes more pronounced with the extension of the π-conjugated system. As expected, **10**, **11** and **12a,b** exhibited more separated HOMO and LUMO electron distributions.

Both the HOMO and LUMO energy values (Figure 8) showed dependence on the electron-donating characteristics of the aminoaryl substituent of the triazoloquinazolines **6a-c**. [1,2,4]Triazolo[1,5-*c*]quinazolines **6b**, **6d** and **6h** with diphenylaminophenyl group demonstrated the lowest energy gap Eg = 3.46–3.48 eV compared to the other compounds of the series **6**. Incorporation of additional phenylene ring influence on both HOMO and LUMO levels and result in reduction of Eg value by 0.43 eV. The trends in the theoretical HOMO and LUMO levels are closely coincident with the UV–Vis absorption data, Table 1. The HOMO levels of 9,9′-spirobisfluoren-substituted triazoloquinazolines **6j**, **12a** and **12b** turned out to be significantly lower than those of their counterparts depicting the weaker electron donating ability of residue at position 5.

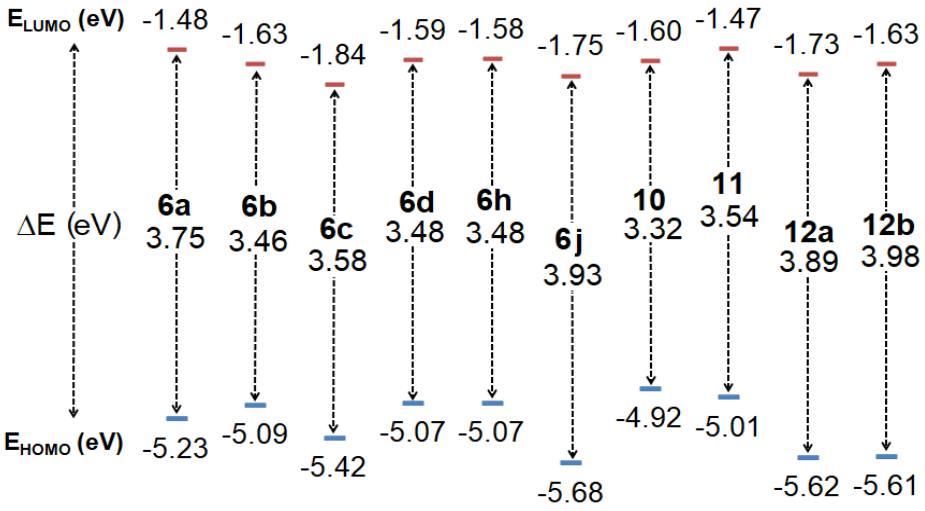

Figure 8. HOMO-LUMO energy levels and Eg for compounds **6a-d**, **6h**, **6j**, **10**, **11** and **12a,b** in gas phase.

Further, the geometries of **6a-d**, **6h**, **6j**, **10**, **11**, and **12a,b** were additionally optimized in toluene and MeCN at both the ground and excited states (Figure S13). Structural changes, including variations in dihedral angles (α), and bond lengths (L) between the donor and acceptor group upon excitation, were analyzed (Table S14). For clarity, dihedral angles were reported in the 0–90° range as absolute values to illustrate deviations from planarity.

The molecular geometries of compounds **6a–c**, which differ only in the nature of the electron-donating fragment, were compared. The rotation angle of the phenyl substituent (α_1) slightly decreases by 3–15° in the excited state compared to the ground state for compounds **6b,c** in both solvents and for **6a** in acetonitrile. At the same time, the bond length L_1 remains unchanged. In contrast, the angle α_2 increases by 0.25–3.21°, which results in a distortion of the triazoloquinazoline core in exited state. The aminoaryl donor fragment is considerably twisted relative to the rest of the molecule in the ground state (angle $\alpha_3 \approx 34.5–55.0°$). This torsion angle considerably reduces in S_1 state in all cases, except for compound **6a** in acetonitrile. In toluene, the angle α_3 does not exceed 4°, and the bond length L_2 shortens by 0.043–0.066 Å, which makes molecular geometry of **6a–c** nearly planar. Notably, the diethylaminophenyl fragment (compound **6a**) remains twisted upon excitation in acetonitrile, while the corresponding bond length does not change, indicating the absence of effective conjugation and intramolecular charge transfer.

The introduction of a substituent into the phenyl ring has practically no effect on the molecular geometry (compounds **6e**, and **6h** respect to **6b**). The geometry changes between the ground and excited states for compound **6j** are similar to those observed for **6b** and **6c**. Compound **10** in toluene is characterized two almost planar conjugated systems—the 2-phenyltriazoloquinazoline core and the aminobiphenyl fragment—rotated relative to each other by approximately 40° (α_3). In acetonitrile,

© 2025 by the author(s). Distributed under a Creative Commons CC BY license.

Preprints.org (www.preprints.org) | NOT PEER-REVIEWED | Posted: 22 October 2025 doi:10.20944/preprints202510.1579.v1

however, the aminobiphenyl moiety adopts a non-planar configuration, suggesting that intramolecular charge transfer is accompanied by a twisted geometry (TICT effect). In compound **11**, the phenyl and biphenyl substituents are arranged nearly parallel to each other (angles α_1 and α_3), but rotated significantly (α_1 and $\alpha_3 > 55°$) relative to the triazoloquinazoline fragment in all states. This distortion arises from steric hindrance imposed by the substituents and correlates with the hypsochromic shift in the absorption spectra. The aminobiphenyl fragment undergoes changes similar to those in compound **10**, and the excited state likely corresponds to analogous conformations.

Interestingly, the 9,9'-spirobifluorene-contained 2-phenyl- and 2-ethyl-[1,2,4]triazolo[1,5-c]quinazolines **12a** and **12b** adopt a more planar molecular configuration of (fluorene)phenyl-[1,2,4]triazolo[1,5-c]quinazoline core in the S_1 state compared to S_0 in both solvents.

3. Materials and Methods

3.1. General Information

Unless otherwise indicated, all common reagents and solvents were obtained from commercial suppliers and used without further purification. Melting points were determined using Boetius combined heating stages. Thin-layer chromatography (TLC) was performed on ALUGRAM Xtra SIL G/UV254 plates (Macherey-Nagel, Germany). ^{1}H NMR and ^{13}C NMR spectra were recorded at room temperature on a Bruker DRX-400 spectrometer (Bruker, Rheinstetten, Germany) operating at 400 and 100 MHz, respectively, using $CDCl_3$ or DMSO-d_6 as solvents. Chemical shifts (δ) are reported in parts per million (ppm) relative to the residual solvent signals as internal standards. Coupling constants (J) are given in Hertz (Hz). The following abbreviations were used to describe the NMR signals: s - singlet, br. s - broad singlet, d - doublet, t - triplet, q - quartet and m - multiplet. Mass spectra were obtained using a Shimadzu GCMS-QP2010 Ultra instrument with electron ionization (EI) (Shimadzu, Duisburg, Germany). Elemental analyses (C, H, N) were carried out on a Perkin–Elmer 2400 elemental analyzer (Perkin–Elmer, Waltham, MA, USA).

3.2. Photophysical Characterization

UV/Vis absorption spectra were recorded on the Shimadzu UV-1800 (Shimadzu, Duisburg, Germany) using quartz cells with 1 cm path length at room temperature. Photoluminescent spectra were measured on the Horiba FluoroMax-4 (HORIBA Ltd., Kyoto, Japan) using quartz cells with 1 cm path length at room temperature. Absolute quantum yields of luminescence of target compounds in solution and solid state were measured using the Integrating Sphere Quanta-φ of the Horiba-Fluoromax-4.

3.3. Crystallography

The single crystal of compound **6g** (colourless prism of 0.41×0.19×0.08 mm), **6j** (yellow plank of 0.45×0.16×0.07 mm), **10** (yellow block of 0.41×0.19×0.06 mm) and compound **12a** (colourless prism of 0.46×0.35×0.15 mm) were used for X-ray analysis. Structural studies of the compounds were performed using equipment available in the Collaborative Access Centre "Spectroscopy and Analysis of the Organic compound" at the Postovsky Institute of the Organic Synthesis, Ural Branch, Russian Academy of Sciences. The X-ray diffraction analysis was performed at room temperature on the Xcalibur 3 diffractometer (Oxford Diffraction). Using Olex2 [28], the structure was solved with the ShelXT structure solution program using Intrinsic Phasing and refined with the ShelXL [29], refinement package using full-matrix Least Squares minimization. All non-hydrogen atoms were refined in an anisotropic approximation; the H-atoms were placed in the calculated positions and refined isotropically in the "rider" model.

The results of X-ray diffraction analysis for compounds **6f**, **6g**, **10** and **12a** were deposited with the Cambridge Crystallographic Data Centre (CCDC 2493884, CCDC 2482936, CCDC 2466809 and CCDC 2466371, respectively). These data are free and can be available at www.ccdc.cam.ac.uk.

Crystal data for **6f** $C_{34}H_{23}N_5 \times CHCl_3$, M = 620.94, monoclinic, a = 7.0774(3) Å, b = 31.3482(12) Å, c = 13.5908(6) Å, $\alpha = 90°$, $\beta = 100.008(5)°$, $\gamma = 90°$, V = 2969.4(2) Å^3, space group $P2_1/n$, Z = 4, μ(Mo Kα) = 0.343 mm^{-1}. On the angles $2.273 < \Theta < 30.851°$, 22547 reflections measured, 8194 unique ($R_{int} = 0.0431$)

© 2025 by the author(s). Distributed under a Creative Commons CC BY license.

Preprints.org (www.preprints.org) | NOT PEER-REVIEWED | Posted: 22 October 2025 doi:10.20944/preprints202510.1579.v1

which were used in all calculations. Goodness to fit at F^2 1.011; the final $R_1 = 0.1627$, $wR_2 = 0.2647$ (all data) and $R_1 = 0.0906$, $wR_2 = 0.2269$ ($I>2\sigma(I)$). Largest diff. peak and hole 0.31 and –0.27 ēÅ^{-3}.

Crystal data for **6g** $C_{29}H_{31}N_5$, M = 449.59, triclinic, a = 6.1850(4) Å, b = 11.2776(8) Å, c = 18.3493(14) Å, $\alpha = 79.834(6)°$, $\beta = 86.369(6)°$, $\gamma = 82.445(6)°$, V = 1247.81(18) Å^3, space group *P -1*, Z = 2, μ(Mo Kα) = 0.072 mm^{-1}. On the angles $2.3280 < \Theta < 25.3610°$, 8878 reflections measured, 6476 unique ($R_{int} = 0.0627$) which were used in all calculations. Goodness to fit at F^2 1.006; the final $R_1 = 0.1704$, $wR_2 = 0.2581$ (all data) and $R_1 = 0.0787$, $wR_2 = 0.1910$ ($I>2\sigma(I)$). Largest diff. peak and hole 0.44 and –0.25 ēÅ^{-3}.

Crystal data for **10** $C_{31}H_{27}N_5$, M = 469.57, monoclinic, a = 11.7244(4) Å, b = 17.3697(8) Å, c = 12.1246(5) Å, $\alpha = 90°$, $\beta = 92.182(4)°$, $\gamma = 90°$, V = 2467.38(17) Å^3, space group $P2_1/n$, Z = 4, μ(Mo Kα) = 0.076 mm^{-1}. On the angles $2.6290 < \Theta < 30.5640°$, 11637 reflections measured, 3574 unique ($R_{int} = 0.0531$) which were used in all calculations. Goodness to fit at F^2 1.002; the final $R_1 = 0.1310$, $wR_2 = 0.1813$ (all data) and $R_1 = 0.0628$, $wR_2 = 0.1429$ ($I>2\sigma(I)$). Largest diff. peak and hole 0.22 and –0.19 ēÅ^{-3}.

Crystal data for **12a** $C_{46}H_{28}N_4 \times 2(CHCl_3)$, M = 875.46, triclinic, a = 11.9241(4) Å, b = 13.3599(6) Å, c = 13.5961(6) Å, $\alpha = 77.308(4)°$, $\beta = 79.548(3)°$, $\gamma = 81.823(3)°$, V = 2066.08(15) Å^3, space group *P -1*, Z = 2, μ(Mo Kα) = 0.457 mm^{-1}. On the angles $2.4850 < \Theta < 30.6010°$, 16932 reflections measured, 6038 unique ($R_{int} = 0.0466$) which were used in all calculations. Goodness to fit at F^2 1.089; the final $R_1 = 0.1361$, $wR_2 = 0.2039$ (all data) and $R_1 = 0.0741$, $wR_2 = 0.2491$ ($I>2\sigma(I)$). Largest diff. peak and hole 0.46 and –0.46 ēÅ^{-3}.

3.4. Quantum-Chemical Calculations

The quantum chemical calculations were carried out at the B3LYP/6-31G*//PM6 level of theory with the help of the Gaussian-09 [30] program package. No symmetry restrictions were applied during the geometry optimization procedure. The solvent effects were taken into account using the SMD (Solvation Model based on Density) continuum solvation model suggested by Truhlar and co-workers [31] for acetonitrile and toluene.

3.5. Synthetic Procedures

3.5.1. Synthesis of the Intermediate Products

Ethyl *N*-(2-cyanophenyl)carbamate (**2**) was prepared similar to describe procedure [17]. To 2-aminobenzonitrile (2.7 g, 22.8 mmol) and potassium carbonate (9.5 g, 68.6 mmol) in tetrahydrofuran (130 ml) ethyl chloroformate (4.4 ml, 46.0 mmol) was added. The mixture was stirred at 85 °C for 16 h. After cooling the precipitate was filtered, washed with tetrahydrofuran and water. Product was used without further purification. Colourless solid, yield: 99% (4.3 g); ^{1}H NMR (DMSO-d$_6$, 400 MHz) δ 1.24 (t, ^3J = 6.8, 3H, CH_3), 4.14 (q, ^3J = 6.8, 2H, CH_2), 7.30–7.34 (m, 1H), 7.50–7.52 (m, 1H), 7.64–7.68 (m, 1H), 7.77–7.79 (m, 1H), 9.7 (s, 1H, NH).

Compounds **4a-c** were obtained following to described procedure [17]. Ethyl *N*-(2-cyanophenyl)carbamate **2** (1.5 g, 7.85 mmol) and corresponding hydrazide **3a-c** (9.36 mmol) were stirred in N,N-dimethylformamide (10 mL) at 120 °C for 12 hours. After cooling water was added to the mixture, precipitated product was filtered off and recrystallized from MeCN (for **4a**) or DMSO (for **4b** and **4c**).

2-Phenyl-[1,2,4]triazolo[1,5-*c*]quinazolin-5(6*H*)-one (**4a**). Colourless solid, yield: 72% (1.5 g); mp 296–298 °C (mp lit. 311–313 °C [32]). ^{1}H NMR (DMSO-d$_6$, 400 MHz) δ 7.39–7.66 (m, 6H), 8.24–8.25 (m, 3H), 12.31 (s, 1H, NH); EIMS (m/z, I_{rel} %): 263 $[M+1]^+$ (18), 262 $[M]^+$ (100); Exact mass for $C_{15}H_{10}N_4O$ (262.0855).

2-(*p*-Tolyl)-[1,2,4]triazolo[1,5-*c*]quinazolin-5(6*H*)-one (**4b**). Colourless solid, yield: 83% (1.80 g); mp 305–307 °C. ^{1}H NMR (DMSO-d$_6$, 400 MHz) δ 2.43 (3H, s, CH_3), 7.32–7.40 (3H, m, H-3′, H-5′, H-8 or H-9), 7.45–7.47 (1H, m, H-7 or H-10), 7.64–7.64 (1H, m, H-8 or H-9), 8.12–8.14 (2H, d, ^3J = 7.5, H-2′, H-6′), 8.22–8.24, (1H, m, H-7 or H-10), 12.28 (1H, s, NH); EIMS (m/z, I_{rel} %): 277 $[M+1]^+$ (20), 276 $[M]^+$ (100); Exact mass for $C_{16}H_{12}N_4O$ (276.1011).

2-4-(*Tert*-butyl)phenyl-[1,2,4]triazolo[1,5-*c*]quinazolin-5(6*H*)-one (**4c**). Colourless solid, yield: 93% (2.33 g); mp 243–245 °C. ^{1}H NMR ($CDCl_3$, 400 MHz) δ 1.37 (9H, s, *t*-Bu), 7.36–7.40 (1H, m, H-8 or

© 2025 by the author(s). Distributed under a Creative Commons CC BY license.

Preprints.org (www.preprints.org) | NOT PEER-REVIEWED | Posted: 22 October 2025 doi:10.20944/preprints202510.1579.v1

H-9), 7.51–7.54 (3H, m, H-3′, H-5′, H-7 or H-10), 7.59–7.61 (1H, m, H-8 or H-9), 8.29–8.31 (2H, d, ^3J = 7.8, H-2′, H-6′), 8.35–8.37, (1H, m, H-7 or H-10), 11.4 (1H, s, NH); EIMS (m/z, I_{rel} %): 318 (29), 304 [M-CH_3+1]$^+$ (23), 303 [M-CH_3]$^+$ (100); Exact mass for $C_{19}H_{18}N_4O$ (318.1950).

Compounds **5a-c** were obtained following to described procedure [17]. To the dried [1,2,4]triazolo[1,5-*c*]quinazolin-5(6*H*)-one **3a-c** (1.14 mmol) in phosphorus(V) oxychloride (7.2 mL, 77 mmol), *N*,*N*-diisopropylethylamine (0.4 mL, 2.27 mmol) was added carefully and the mixture was stirred for 20 h at 110 °C. Condenser was equipped with a calcium chloride drying tube. The mixture was concentrated. Resulting product was purified with column chromatography on SiO_2 using mixture of hexane and EtOAc as eluent.

5-Chloro-2-phenyl-[1,2,4]triazolo[1,5-*c*]quinazoline (**5a**). Colourless solid, yield: 94% (300 mg); mp 170–172 °C. ^{1}H NMR ($CDCl_3$, 400 MHz): δ 7.53–7.55 (3H, m, H-3′, H-4′, H-5′), 7.75–7.79 (1H, m, H-8 or H-9), 7.85–7.89 (1H, m, H-8 or H-9), 8.01–8.02 (1H, m, H-10), 8.39–8.42 (2H, m, H-2′, H-6′), 8.61 (1H, d, ^3J = 7.9, H-7). EIMS (m/z, I_{rel} %): 282 [M + 2]$^+$ (33), 281 [M+1]$^+$ (21), 280 [M]$^+$ (100), 245 (18), 163 (18), 102 (15), 89 (15). Exact mass for $C_{15}H_9ClN_4$ (280.0516).

5-Chloro-2-(*p*-tolyl)-[1,2,4]triazolo[1,5-*c*]quinazoline (**5b**). Beige solid, yield: 82% (277 mg); mp 166–168 °C. ^{1}H NMR (DMSO-d_6, 400 MHz): δ 2.45 (s, 3H, CH_3), 7.38 (2H, d, ^3J = 8.1, H-3′, H-5′), 7.84–7.88 (1H, m, H-8 or H-9), 7.94–7.98 (1H, m, H-8 or H-9), 8.01–8.03 (1H, m, H-10), 8.22 (2H, d, ^3J = 8.1, H-2′, H-6′), 8.54 (1H, d, ^3J = 7.8, H-7); EIMS (m/z, I_{rel} %): 296 [M+2]$^+$ (35), 295 [M+1]$^+$ (25), 294 [M]$^+$ (100), 293 (17), 163 (11), 131 (13), 116 (12), 102 (19), 90 (13); Exact mass for $C_{16}H_{11}ClN_4$ (294.0672).

5-Chloro-2-(4-(*Tert*-butyl)phenyl)-[1,2,4]triazolo[1,5-*c*]quinazoline (**5c**). Beige solid, yield: 80% (297 mg); mp 126–128 °C. ^{1}H NMR (DMSO-d_6, 400 MHz): δ 1.39 (s, 9H, 3 CH_3), 7.56 (2H, d, ^3J = 8.5, H-3′, H-5′), 7.82–7.86 (1H, m, H-8 or H-9), 7.93–7.95 (1H, m, H-8 or H-9), 7.99–8.01 (1H, m, H-10), 8.22 (2H, d, ^3J = 8.5, H-2′, H-6′), 8.54 (1H, d, ^3J = 7.9, H-7); EIMS (m/z, I_{rel} %): 338 [M+2]$^+$ (10), 336 [M]$^+$ (28), 323 (35), 322 (23), 321 [M-CH_3]$^+$ (100), 163 (11), 146 (13), 102 (11); Exact mass for $C_{19}H_{17}ClN_4$ (336.1142).

4-Hydrazino-2-(4-bromophenyl)quinazoline (**7**) and 5-(4-Bromophenyl)-2-ethyl-[1,2,4]triazolo[1,5-*c*]quinazoline (**8b**) were prepared as described previously [8,9].

Synthesis of 5-(4-Bromophenyl)-2-phenyl-[1,2,4]triazolo[1,5-*c*]quinazoline (**8a**).

Method 1. In a round-bottom flask equipped with a magnetic stirred bar, 4-hydrazino-2-(4-bromophenyl)quinazoline **7** (0.27 g, 0.86 mmol) in glacial acetic acid (7 mL) triethyl orthobenzoate (0.86 mL, 4.3 mmol) were added. The mixture was refluxed for 16 h. After cooling down the water was added until the formation of precipitate. The product was filtered off and washed with water and recrystallized from DMSO.

Method 2. In a round-bottom flask equipped with a magnetic stirred bar, 5-(4-Bromophenyl)-3-phenyl-[1,2,4]triazolo[4,3-*c*]quinazoline **9** (0.18 g, 0.45 mmol) refluxed in glacial acetic acid (3.6 mL) for 20 h. After cooling down the water was added until the formation of precipitate. The solid was filtered off and washed with water.

Colourless powder, yield 79%, 0.27 g (method 1), yield 48%, 0,073 g (method 2); mp 190–192 °C; ^{1}H NMR (DMSO-d_6, 400 MHz) δ 7.58–7.60 (3H, m, H-3′, H-4′, H-5′), 7.85–7.91 (3H, m, H-3′′, H-5′′, H-8 or H-9), 7.96–7.99 (1H, m, H-8 or H-9), 8.13–8.15 (1H, m, H-10), 8.30–8.33 (2H, m, H-2′, H-6′), 8.53–8.55 (3H, m, H-2′′, H-6′′, H-7); ^{13}C {^{1}H} NMR ($CDCl_3$, 100 MHz, 45 °C) δ 116.9, 123.3, 125.4, 127.1, 128.4, 128.8, 128.9, 129.7, 130.6, 131.3, 132.2, 132.5, 142.2, 145.0, 152.4, 162.8; EIMS (m/z, I_{rel} %): 402 [M+2]$^+$ (100), 401 [M+1]$^+$ (66), 400 [M]$^+$ (99); Exact mass for $C_{21}H_{13}BrN_4$ (400.0324).

Synthesis of 5-(4-Bromophenyl)-3-phenyl-[1,2,4]triazolo[4,3-*c*]quinazoline (**9**). Starting 2-(4-bromophenyl)-4-hydrazinoquinazoline was preliminarily dried in oven at 100 °C for 4 h.

Method 1. In a round-bottom flask equipped with a magnetic stirred bar, 2-(4-bromophenyl)-4-hydrazinoquinazoline **7** (0.32 g, 1.00 mmol) in absolute ethanol (17 mL) and triethyl orthobenzoate (1 mL, 4.80 mmol) were added. The mixture was refluxed for 4 h. Condenser was equipped with a calcium chloride drying tube. After cooling down and partial evaporation the solid was filtered off, washed with EtOH (5 mL). The product was purified by column chromatography on SiO_2 using EtOAc and hexane as eluent, gradually from (1:9) to pure EtOAc.

Method 2. In a round-bottom flask equipped with a magnetic stirred bar, dried 2-(4-bromophenyl)-4-hydrazinoquinazoline 7 (0.20 g, 0.62 mmol) and triethyl orthobenzoate (1 mL, 4.80

© 2025 by the author(s). Distributed under a Creative Commons CC BY license.

Preprints.org (www.preprints.org) | NOT PEER-REVIEWED | Posted: 22 October 2025 doi:10.20944/preprints202510.1579.v1

mmol) were added. The mixture was refluxed for 4 h. A condenser was equipped with a calcium chloride drying tube. After cooling down the solid was filtered off, washed with EtOH (5 mL) and dried.

Colourless powder, yield 63% (method 1), yield 81% (method 2); mp 237–239 °C; ^{1}H NMR (DMSO-d$_6$, 400 MHz) δ 7.13–7.23 (6H, m, H-2'', H-3'', H-5'', H-6'', H-2', H-6'), 7.29–7.31 (3H, m, H-3', H-4', H-5'), 7.78–7.82 (1H, m, H-7 or H-10), 7.84–7.88 (1H, m, H-7 or H-10), 7.96–7.98 (1H, m, H-10), 8.62 (1H, d, ^3J = 7.9, H-7); EIMS (m/z, I_{rel} %): 402 $[M+2]^+$ (94), 401 $[M+1]^+$ (79), 400 $[M]^+$ (100); Exact mass for $C_{21}H_{13}BrN_4$ (400.0324).

3.5.1. Synthesis of the Target Products

General cross-coupling procedure for the synthesis of compounds **6a-j**, **10**, **11** and **12a,b.**

The corresponding boronic acid or boronic acid pinacol ester (0.57 mmol), $PdCl_2(PPh_3)_2$ (40 mg, 57 μmol), PPh_3 (30 mg, 114 μmol), saturated solution of K_2CO_3 (3.1 mL) and EtOH (3.1 mL) were added to the suspension of the corresponding chloro or bromo derivative (**5a-c** or **8a,b**, **9**) (0.53 mmol) in toluene (19 mL). The mixture was stirred at 85 °C for 14–30 h in argon atmosphere in round-bottom pressure flask equipped with magnetic stirred bar. The reaction mixture was cooled to room temperature, and EtOAc/H_2O (10/10 mL) mixture was added. The organic layer was separated, additionally washed with water (10 mL), and evaporated at reduced pressure. The product was purified by column chromatography.

5-(4-Diethylaminophenyl)-2-phenyl-[1,2,4]triazolo[1,5-*c*]quinazoline (**6a**).

The general procedure was applied using 5-chloro-2-phenyl- [1,2,4]triazolo[1,5-*c*]quinazoline **5a** and 4-(diethylamino)phenylboronic acid as the starting materials. Reaction time is 30 h. Column chromatography: SiO_2, EtOAc and hexane (1:9) was used as an eluent. Pale-yellow solid, yield: 54% (114 mg); mp = 135–137 °C; ^{1}H NMR ($CDCl_3$, 400 MHz): δ 1.27 (6H, t, ^3J = 7.1, 2CH_3), 3.50 (4H, q, ^3J = 7.1, 2CH_2), 6.85 (2H, d, ^3J = 9.2, H-3'', H-5''), 7.47–7.56 (3H, m, H-3', H-4', H-5'), 7.60–7.64 (1H, m, H-8), 7.77–7.81 (1H, m, H-9), 8.04–8.05 (1H, m, H-10), 8.43–8.45 (2H, m, H-2', H-6'), 8.59 (1H, d, ^3J = 8.1, H-7), 8.74 (2H, d, ^3J = 9.2, H-2'', H-6''); ^{13}C {^{1}H} NMR ($CDCl_3$, 100 MHz) δ 12.8 (2 CH_3), 44.7 (2 CH_2), 110.8, 116.9, 118.0, 123.8, 127.0, 127.8, 128.3, 128.8, 130.3, 130.8, 131.9, 132.5, 143.6, 146.8, 150.2, 153.2, 163.7; EIMS (m/z, I_{rel} %): 394 $[M+1]^+$ (18), 393 $[M]^+$ (58), 379 (29), 378 $[M-CH_3]^+$ (100), 350 (12), 189 (17); Exact mass for $C_{25}H_{23}N_5$ (393.1953). Calcd: C, 76.31, H, 5.89, N, 17.80%; Found: C, 76.22, H, 6.04, N, 17.56%.

5-(4-Diphenylaminophenyl)-2-phenyl-[1,2,4]triazolo[1,5-*c*]quinazoline (**6b**). The general procedure was applied using 5-chloro-2-phenyl-[1,2,4]triazolo[1,5-*c*]quinazoline **5a** and 4-(diphenylamino)phenylboronyc acid as the starting materials. Reaction time is 14 h. Column chromatography: SiO_2, hexane and CH_2Cl_2 (7:3) and then EtOAc and hexane (1:9). Pale-yellow solid, yield: 58% (150 mg); mp = 191–193 °C; ^{1}H NMR ($CDCl_3$, 400 MHz) δ 7.13–7.16 (2H, m, Phenyl), 7.21–7.24 (6H, m, Phenyl, H-3'', H-5''), 7.33–7.37 (4H, m, Phenyl), 7.51–7.53 (3H, m, H-3', H-4', H-5'), 7.66–7.70 (1H, m, H-8), 7.81–7.84 (1H, H-9), 8.08 (1H, d, ^3J = 8.2, H-10), 8.38–8.44 (2H, m, H-2', H-6'), 8.61–8.65 (3H, m, H-7, H-2'', H-6''); EIMS (m/z, I_{rel} %): 490 $[M+1]^+$ (39), 489 $[M]^+$ (100), 488 (14), 77 (11); ^{13}C {^{1}H} NMR ($CDCl_3$, 100 MHz) δ 117.2, 120.8, 123.9, 124.1, 124.4, 125.9, 127.8, 128.6, 128.8, 129.7, 130.5, 130.6, 131.9, 132.1, 143.3, 146.2, 147.0, 151.1, 153.2, 164.0; Exact mass for $C_{33}H_{23}N_5$ (489.1953). Calcd: C, 80.96, H, 4.74, N, 14.30%. Found: C, 80.86, H, 4.87, N, 14.19%.

5-(4-(9*H*-carbazol-9-yl)phenyl)-2-phenyl-[1,2,4]triazolo[1,5-*c*]quinazoline (**6c**).

The general procedure was applied using 5-chloro-2-phenyl- [1,2,4]triazolo[1,5-*c*]quinazoline **5a** and 9*H*-Carbazole-9-(4-phenyl) boronic acid pinacol ester as the starting materials. Reaction time is 21 h. Column chromatography: SiO_2, hexane and CH_2Cl_2 (7:3) and then EtOAc and hexane (1:9). Pale-yellow solid, yield: 44% (113 mg); mp = 235–237 °C; ^{1}H NMR ($CDCl_3$, 400 MHz) δ 7.33–7.36 (2H, m, carbazolyl), 7.46–7.49 (2H, m, carbazolyl), 7.53–7.57 (3H, m, H-3', H-4, H-5'), 7.61–7.63 (2H, m, carbazolyl), 7.75–7.79 (1H, m, H-8), 7.87–7.90 (3H, m, H-9, H-3'', H-5''), 8.17–8.19 (3H, m, H-10, carbazolyl), 8.46–8.48 (2H, m, H-2', H-6'), 8.69 (1H, d, ^3J = 8.2, H-7), 8.98–99.00 (2H, m, H-2'', H-6''); ^{13}C {^{1}H} NMR ($CDCl_3$, 100 MHz) δ 110.1, 117.6, 120.6, 120.6, 123.9, 124.1, 126.3, 126.6, 127.9, 128.6, 129.0, 130.4, 130.6, 130.8, 132.4, 140.6, 141.0, 143.1, 145.7, 153.2, 164.4; EIMS (m/z, I_{rel} %): 488 $[M+1]^+$

© 2025 by the author(s). Distributed under a Creative Commons CC BY license.

Preprints.org (www.preprints.org) | NOT PEER-REVIEWED | Posted: 22 October 2025 doi:10.20944/preprints202510.1579.v1

(37), 487 $[M]^+$ (100). Exact mass for $C_{33}H_{21}N_5$ (487.1797). Calcd: C, 81.29; H, 4.34; N, 14.37%. Found: C, 81.21; H, 4.42; N, 14.28%.

5-(4-Dimethylaminophenyl)-2-(*p*-tolyl)-[1,2,4]triazolo[1,5-*c*]quinazoline (**6d**). The general procedure was applied using 5-chloro-2-(*p*-tolyl)-[1,2,4]triazolo[1,5-*c*]quinazoline **5b** and 4-(dimetylamino)phenylboronyc acid as the starting materials. Reaction time is 21 h. Column chromatography: SiO_2, hexane and CH_2Cl_2 (1:1) and then EtOAc and hexane (1:9). Colourless solid, yield: 56% (112 mg); mp = 176–178 °C; ^{1}H NMR (400 MHz, $CDCl_3$): δ 2.45 (3H, s, CH_3), 3.12 (6H, s, $N(CH_3)_2$), 6.88 (2H, d, ^3J = 9.2, H-3'', H-5''), 7.34 (2H, d, ^3J = 8.0, H-3', H-5'), 7.61–7.65 (1H, m, H-8), 7.77–7.81 (1H, m, H-9), 8.04–8.06 (1H, m, H-10), 8.32 (2H, d, ^3J = 8.0, H-2', H-6'), 8.58 (1H, d, ^3J = 8.0, H-7), 8.74–8.77 (2H, m, H-2'', H-6''); ^{13}C {^{1}H} NMR ($CDCl_3$, 100 MHz) δ 21.7 (CH_3), 40.3 ($N(CH_3)_2$), 111.3, 117.0, 119.0, 123.8, 127.1, 127.7, 128.0, 128.3, 129.5, 131.8, 132.3, 140.5, 143.6, 146.8, 152.6, 153.1, 163.8; EIMS (m/z, I_{rel} %): 380 $[M + 1]^+$ (28), 379 $[M]^+$ (100), 378 (29), 190 (10); Exact mass for $C_{24}H_{21}N_5$ (379.1797). Calcd: C, 75.97, H, 5.58, N, 18.45%. Found: C, 75.92, H, 5.63, N, 18.58%.

5-(4-Diphenylaminophenyl)-2-(*p*-tolyl)-[1,2,4]triazolo[1,5-*c*]quinazoline (**6e**). The general procedure was applied using 5-chloro-2-(*p*-tolyl)-[1,2,4]triazolo[1,5-*c*]quinazoline **5b** and 4-(diphenylamino)phenylboronyc acid as the starting materials. Reaction time is 21 h. Column chromatography: SiO_2, hexane and CH_2Cl_2 (1:4) and then EtOAc and hexane (1:9). Pale-yellow, yield: 27% (73 mg); mp = 198–200 °C; ^{1}H NMR ($CDCl_3$, 400 MHz): 2.44 (3H, s, CH_3), 7.12–7.16 (2H, m, Phenyl), 7.20–7.25 (6H, m, Phenyl, H-3'', H-5''), 7.31–7.36 (6H, m, Phenyl, H-3', H-5'), 7.65–7.69 (1H, m, H-8), 7.79–7.84 (1H, m, H-9), 8.06–8.08 (1H, m, H-10), 8.29 (2H, d, ^3J = 8.1, H-2', H-6'), 8.60–8.65 (3H, m, H-7, H-2'', H-6''); ^{13}C {^{1}H} NMR ($CDCl_3$, 100 MHz) δ 21.7 (CH_3), 117.2, 120.8, 123.9, 124.2, 124.4, 125.9, 127.7, 127.8, 128.6, 129.6, 129.7, 131.9, 132.0, 140.7, 143.3, 146.2, 147.0, 151.0, 153.1, 164.1; EIMS (m/z, I_{rel} %): 504 $[M+1]^+$ (40), 503 $[M]^+$ (100), 502 (13), 252 (11), 77 (11); Exact mass for $C_{34}H_{25}N_5$ (503.2110). Calcd: C, 81.09, H, 5.00, N, 13.91%. Found: C, 81.55, H, 5.13, N, 13.32%.

5-(4-(9*H*-carbazol-9-yl)phenyl)-2-(*p*-tolyl)-[1,2,4]triazolo[1,5-*c*]quinazoline (**6f**). The general procedure was applied using 5-chloro-2-(*p*-tolyl)-[1,2,4]triazolo[1,5-*c*]quinazoline **5b** and 9*H*-Carbazole-9-(4-phenyl) boronic acid pinacol ester as the starting materials. Reaction time is 21 h. Column chromatography: SiO_2, hexane and CH_2Cl_2 (7:3). Colourless solid, yield: 70% (187 mg); mp = 210–212 °C; ^{1}H NMR ($CDCl_3$, 400 MHz): 2.46 (3H, s, CH_3), 7.33–7.38 (4H, m, carbazolyl, H-3', H-5'), 7.46–7.50 (2H, m, carbazolyl), 7.61–7.63 (2H, m, carbazolyl), 7.75–7.79 (1H, m, H-8), 7.87–7.92 (3H, m, H-9, H-3'', H-5''), 8.16–8.19 (3H, m, H-10, carbazolyl), 8.35 (d, ^3J = 8.1, 2H, H-2', H-6'), 8.67–8.69 (1H, m, H-7), 8.97–9.01 (2H, m, H-2'', H-6''); ^{13}C {^{1}H} NMR ($CDCl_3$, 100 MHz) δ 21.7 (CH_3), 110.1, 117.6, 120.6, 120.6, 123.9, 124.1, 126.3, 126.6, 127.6, 127.8, 128.5, 128.9, 129.7, 130.7, 132.3, 132.4, 140.6, 140.9, 141.0, 143.1, 145.7, 153.2, 164.5; EIMS (m/z, I_{rel} %): 502 $[M+1]^+$ (38), 501 $[M]^+$ (100), 500 (13), 251 (19); Exact mass for $C_{34}H_{23}N_5$ (501.1953). Calcd: C, 81.42, H, 4.62, N, 13.96%. Found: C, 81.29, H, 4.70, N, 13.83%.

5-(4-Diethylaminophenyl)-2-(4-(*tert*-butyl)phenyl)-[1,2,4]triazolo[1,5-*c*]quinazoline (**6g**). The general procedure was applied using 5-chloro-2-(4-(*tert*-butyl)phenyl)-[1,2,4]triazolo[1,5-*c*]quinazoline **5c** and 4-(diethylamino)phenyl boronic acid as the starting materials. Reaction time is 14 h. Column chromatography: SiO_2, eluent: gradually from hexane/CH_2Cl_2 (8:2) to CH_2Cl_2. Yellow solid, yield: 20% (46 mg); mp = 135–137 °C; ^{1}H NMR ($CDCl_3$, 400 MHz): δ 1.27 (6H, t, ^3J = 7.1, $2CH_3$), 1.39 (9H, s, *t*-Bu), 3.50 (4H, q, ^3J = 7.1, $2CH_2$), 6.84 (2H, d, ^3J = 9.1, H-3'', H-5''), 7.55 (2H, d, ^3J = 8.4, H-3', H-5'), 7.60–7.63 (1H, m, H-8), 7.76–7.80 (1H, m, H-9), 8.03–8.05 (1H, m, H-10), 8.35 (2H, d, ^3J = 8.4, H-2', H-6'), 8.59 (1H, d, ^3J = 8.4, H-7), 8.74 (2H, d, ^3J = 9.1, H-2'', H-6''); ^{13}C {^{1}H} NMR ($CDCl_3$, 100 MHz) δ 12.7 ($2CH_3$), 31.3 ($C(\underline{C}H_3)_3$), 34.9 ($\underline{C}(CH_3)_3$), 44.6 (2 CH_2), 110.7, 116.8, 117.9, 123.7, 125.6, 126.8, 127.4, 127.9, 128.1, 131.7, 132.4, 143.5, 146.7, 150.1, 153.0, 153.5, 163.6; EIMS (m/z, I_{rel} %): 450 $[M+1]^+$ (26), 449 $[M]^+$ (72), 435 (36), 434 $[M\text{-}CH_3]^+$ (100), 390 (14), 210 (27), 196 (14), 182 (11); Exact mass for $C_{29}H_{31}N_5$ (449.2579). Calcd: C, 77.47, H, 6.95, N, 15.58%; Found: C, 77.38, H, 6.85, N, 15.44%.

5-(4-Diphenylaminophenyl)-2-(4-(*tert*-butyl)phenyl)-[1,2,4]triazolo[1,5-*c*]quinazoline (**6h**). The general procedure was applied using 5-chloro-2-(4-(*tert*-butyl)phenyl)-[1,2,4]triazolo[1,5-*c*]quinazoline **5c** and 4-(diphenylamino)phenylboronyc acid as the starting materials. Reaction time is 14 h. Column chromatography: SiO_2, hexane and CH_2Cl_2 (7:3) and then EtOAc and hexane (1:9). Pale-yellow solid, yield: 61% (177 mg); mp = 223–225 °C; ^{1}H NMR ($CDCl_3$, 400 MHz): δ 1.38 (9H, s, *t*-

© 2025 by the author(s). Distributed under a Creative Commons CC BY license.

Preprints.org (www.preprints.org) | NOT PEER-REVIEWED | Posted: 22 October 2025 doi:10.20944/preprints202510.1579.v1

Bu), 7.12–7.16 (2H, m, Phenyl), 7.20–7.24 (6H, m, Phenyl, H-3'', H-5''), 7.33–7.37 (4H, m, Phenyl), 7.54 (2H, d, ^3J = 8.3, H-3', H-5'), 7.66–7.69 (1H, m, H-8), 7.80–7.84 (1H, m, H-9), 8.06–8.08 (1H, m, H-10), 8.32 (2H, d, ^3J = 8.3, H-2', H-6'), 8.61–8.65 (3H, m, H-7, H-2'', H-6''); ^{13}C {^{1}H} NMR ($CDCl_3$, 100 MHz) δ 31.4 (C($\underline{C}H_3$)$_3$), 35.0 ($\underline{C}$(CH_3)$_3$), 117.3, 120.8, 123.9, 124.3, 124.4, 125.8, 125.9, 127.6, 127.7, 127.8, 128.6, 129.7, 131.9, 132.0, 143.3, 146.2, 147.0, 151.0, 153.1, 153.8, 164.1; EIMS (m/z, I_{rel} %): 546 [M + 1]$^+$ (43), 545 [M]$^+$ (100), 530 [M-CH_3]$^+$ (15), 265 (22), 251 (11); Exact mass for $C_{37}H_{31}N_5$ (545.2579). Calcd: C, 81.44, H, 5.73, N, 12.83%. Found: C, 81.50, H, 5.82, N, 12.78%.

5-(4-(9*H*-carbazol-9-yl)phenyl)-2-(4-(*tert*-butyl)phenyl)-[1,2,4]triazolo[1,5-*c*]quinazoline (**6i**). The general procedure was applied using 5-chloro-2-(4-(*tert*-butyl)phenyl)-[1,2,4]triazolo[1,5-*c*]quinazoline **5c** and 9*H*-Carbazole-9-(4-phenyl) boronic acid pinacol ester as the starting materials. Reaction tyme is 21 h. Column chromatography: SiO_2, hexane and CH_2Cl_2 (7:3) and then EtOAc and hexane (1:9). Colourless solid, yield: 58% (167 mg); mp = 228–230 °C; ^{1}H NMR ($CDCl_3$, 400 MHz): δ 1.40 (9H, s, *t*-Bu), 7.33–7.37 (2H, m, carbazolyl), 7.46–7.50 (2H, m, carbazolyl), 7.58–7.63 (4H, m, carbazolyl, H-3', H-5'), 7.75–7.79 (1H, m, H-8), 7.86–7.92 (3H, m, H-9, H-3'', H-5''), 8.16–8.19 (3H, m, H-10, carbazolyl), 8.38 (2H, d, ^3J = 8.5, H-2', H-6'), 8.68–8.71 (1H, m, H-7), 9.00 (2H, m, ^3J = 8.7, H-2'', H-6''); ^{13}C {^{1}H} NMR ($CDCl_3$, 100 MHz) δ 31.4 (C($\underline{C}H_3$)$_3$), 35.1 ($\underline{C}$(CH_3)$_3$), 110.1, 117.6, 120.6, 120.6, 123.9, 124.1, 125.9, 126.3, 126.6, 127.6, 127.7, 128.5, 128.9, 132.3, 132.4, 140.6, 140.9, 143.1, 145.7, 153.2, 154.1, 164.5; EIMS (m/z, I_{rel} %): 544 [M + 1]$^+$ (44), 543 [M]$^+$ (100), 529 (15), 528 [M-CH_3]$^+$ (36), 268 (13), 264 (27), 250 (19); Exact mass for $C_{37}H_{29}N_5$ (543.2423). Calcd: C, 81.74, H, 5.38, N, 12.88%. Found: C, 81.88, H, 5.46, N, 12.65%.

5-(9,9'-Spirobi[fluoren]-2-yl)-2-phenyl-[1,2,4]triazolo[1,5-*c*]quinazoline (**6j**). The general procedure was applied using 5-chloro-2-phenyl-[1,2,4]triazolo[1,5-*c*]quinazoline **5a** and 9,9'-spirobifluorene-2-boronic acid as the starting materials. Reaction time is 14 h. Column chromatography: SiO_2, hexane and EtOAc (8:2) to pure EtOAc. Colourless solid, yield: 52% (155 mg); mp = 269–271 °C; ^{1}H NMR ($CDCl_3$, 400 MHz) δ 6.86–6.88 (3H, m, fluoren), 7.17–7.24 (3H, m), 7.42–7.47 (6H, m, H-3', H-4', H-5'), 7.64–7.68 (1H, m, H-8), 7.78–7.80 (1H, m, H-9), 7.88–7.90 (2H, m), 7.97–7.8.15 (5H, m), 8.15 (1H, d, ^4J = 1.1, bisfluorenyl), 8.54–8.56 (2H, m, H-2', H-6'); ^{13}C {^{1}H} NMR ($CDCl_3$, 100 MHz) δ 117.3, 120.2, 120.3, 121.0, 123.9, 124.4, 124.5, 126.9, 127.6, 128.0, 128.1, 128.2, 128.8, 128.8, 129.0, 130.2, 130.4, 130.5, 131.0, 132.1, 141.1, 142.1, 143.1, 145.1, 146.5, 148.3, 148.8, 149.8, 152.8, 163.7; EIMS (m/z, I_{rel} %): 561 [M+1]+ (48), 560 [M]$^+$ (100); Exact mass for $C_{40}H_{24}N_4$ (560.2001). Calcd: C, 85.69, H, 4.31, N, 9.99%. Found: C, 85.52, H, 4.45, N, 9.84%.

5-(4'-Diethylamino-[1,1']-biphenyl-4-yl)-2-phenyl-[1,2,4]triazolo[1,5-*c*]quinazoline (**10**). The general procedure was applied using 5-(4-bromophenyl)-2-phenyl-[1,2,4]triazolo[1,5-*c*]quinazoline **8a** and 4-(diethylamino)phenyl boronic acid as the starting materials. Reaction time is 16 h. Column chromatography: SiO_2, hexane and EtOAc from (1:9) to (1:1). Bright yellow solid, yield: 36% (91 mg); mp = 190–192 °C; ^{1}H NMR ($CDCl_3$, 400 MHz): δ 1.23 (6H, t, ^3J = 7.1, 2CH_3), 3.44 (4H, q, ^3J = 7.1, 2CH_2) 6.80 (2H, d, ^3J = 8.3, $Et_2NC_6H_4$), 7.49–7.56 (3H, m, H-3', H-4', H-5'), 7.64 (2H, d, ^3J = 8.3, 2H, $Et_2NC_6H_4$), 7.70–7.73 (1H, m, H-8), 7.81–7.87 (3H, m, H-9, H-3'', H-5''), 8.12–8.14 (1H, m, H-10), 8.44 (2H, d, ^3J = 7.1, H-2', H-6'), 8.65 (1H, d, ^3J = 8.3, H-7), 8.75 (2H, d, ^3J = 8.3, H-2'', H-6''); ^{13}C {^{1}H} NMR ($CDCl_3$, 100 MHz) δ 12.8 (2CH_3), 44.6 (2CH_2), 112.0, 117.4, 123.9, 125.8, 126.7, 127.9, 128.1, 128.3, 128.8, 128.9, 129.0, 130.5, 130.6, 131.1, 132.1, 143.3, 144.5, 146.6, 147.9, 153.1, 164.1; EIMS (m/z, I_{rel} %): 470 [M + 1]$^+$ (34), 469 [M]$^+$ (88), 455 (36), 554 [M-CH_3]$^+$ (100); Exact mass for $C_{31}H_{27}N_5$ (469.2266). Calcd: C, 79.29; H, 5.80; N, 14.91%. Found: C, 79.21, H, 5.93, N, 14.85%.

5-(4'-Diethylamino-[1,1']-biphenyl-4-yl)-3-phenyl-[1,2,4]triazolo[4,3-*c*]quinazoline (**11**). The general procedure was applied using 5-(4-bromophenyl)-3-phenyl- [1,2,4]triazolo[4,3-*c*]quinazoline **9** and 4-(diethylamino)phenyl boronic acid as the starting materials. Reaction time is 11 h. Column chromatography: SiO_2, hexane and EtOAc (1:1) with addition of CF_3COOH and then Et_3N. Pale yellow solid, yield: 20% (38 mg); mp = 175–177 °C; ^{1}H NMR ($CDCl_3$, 400 MHz): δ 1.21 (6H, t, ^3J = 7.1, 2CH_3), 3.41 (4H, q, ^3J = 7.1, 2CH_2) 6.74 (2H, d, ^3J = 8.2, $Et_2NC_6H_4$), 7.08–7.11 (2H, m), 7.19–7.24 (5H, m), 7.29–7.31 (2H, m), 7.35 (2H, d, ^3J = 8.4), 8.72–8.76 (1H, m, H-8), 8.80–8.83 (1H, m, H-9), 8.04–8.06 (1H, m, H-10), 8.75 (1H, d, ^3J = 8.2, H-7); ^{13}C {^{1}H} NMR ($CDCl_3$, 100 MHz) δ 12.8 (2CH_3), 44.6 (2CH_2), 111.9, 116.5, 123.6, 125.3, 126.6, 127.9, 127.9, 128.1, 128.4, 129.1, 129.3, 129.5, 129.8, 131.9, 141.4, 143.6, 146.0, 147.8, 149.2, 150.2; EIMS (m/z, I_{rel} %): 470 [M + 1]$^+$ (30), 469 [M]+ (78), 455 (37), 554 [M-CH_3]$^+$

© 2025 by the author(s). Distributed under a Creative Commons CC BY license.

Preprints.org (www.preprints.org) | NOT PEER-REVIEWED | Posted: 22 October 2025 doi:10.20944/preprints202510.1579.v1

(100); Exact mass for $C_{31}H_{27}N_5$ (469.2266). Calcd: C, 79.29; H, 5.80; N, 14.91%. Found: C, 79.23, H, 5.91, N, 14.86%.

5-(4-(9,9'-Spirobi[fluoren]-2-yl)phenyl)-2-phenyl-[1,2,4]triazolo[1,5-*c*]quinazoline (**12a**). The general procedure was applied using 5-(4-bromophenyl)-2-phenyl- [1,2,4]triazolo[1,5-*c*]quinazoline **8a** and 9,9'-spirobifluorene-2-boronic acid as the starting materials. Reaction time is 14 h. Column chromatography: SiO_2, EtOAc and petroleum ether from (2:8) to (3:1). Pale yellow solid, yield: 83% (75 mg); mp = 175–177 °C; ^{1}H NMR (DMSO-d_6, 400 MHz) δ 6.62–6.64 (1H, m), 6.70–6.72 (2H, m), 7.02 (1H, d, ^4J = 1.0, spirobifluorene) 7.16–7.20 (3H, m), 7.42–7.44 (3H, m), 7.56–7.58 (3H, m), 7.77–7.82 (3H, m), 7.94–7.97 (2H, m), 8.08–8.12 (4H, m), 8.20–8.22 (1H, m), 8.30–8.32 (3H, m), 8.53 (1H, d, ^3J = 8.2, H-7), 8.63 (2H, d, ^3J = 8.7, H-2'', H-6''); ^{13}C {^{1}H} NMR ($CDCl_3$, 100 MHz) δ 117.5, 120.2,120.4, 120.6, 123.0, 123.9, 124.2, 124.3, 127.0, 127.2, 127.8, 128.0, 128.1, 128.2, 128.8, 128.9, 130.4, 130.5, 130.6, 131.0, 132.1, 140.0, 141.3, 142.0, 143.1, 144.0, 146.2, 148.8, 149.4, 149.9, 153.1, 164.1; EIMS (m/z, I_{rel} %): 637 $[M+1]^+$ (50), 636 $[M]^+$ (100); Exact mass for $C_{37}H_{29}N_5$ (636.2314). Calcd: C, 81.74, H, 5.38, N, 12.88%. Found: C, 81.86, H, 5.47, N, 12.63%.

5-(4-(9,9'-Spirobi[fluoren]-2-yl)phenyl)-2-ethyl-[1,2,4]triazolo[1,5-*c*]quinazoline (**12b**). The general procedure was applied using 5-(4-bromophenyl)-2-ethyl-[1,2,4]triazolo[1,5-*c*]quinazoline **8b** (0.12 g, 0.34 mmol) and 9,9'-spirobifluorene-2-boronic acid as the starting materials. Reaction time is 14 h. Column chromatography: SiO_2, hexane and EtOAc (2:8). Colourless solid, yield: 33% (65 mg); mp = 289–291 °C; ^{1}H NMR ($CDCl_3$, 400 MHz) δ 1.46 (3H, t, ^3J = 8.1, CH_3), 3.03 (2H, q, ^3J = 8.1, CH_2), 6.75—6.77 (1H, m), 6.79–6.81 (2H, m), 7.05 (1H, d, ^4J = 1.1, spirobifluorene) 7.12–7.16 (3H, m), 7.38–7.41 (3H, m), 7.64–7.69 (3H, m), 7.72–7.75 (1H, m), 7.79–7.83 (1H, m), 7.87–7.91 (3H, m), 7.95–7.97 (1H, m), 8.07–8.09 (1H, m), 8.52 (1H, d, ^3J = 8.3, H-7), 8.56 (2H, d, ^3J = 8.8, H-2'', H-6''); ^{13}C {^{1}H} NMR ($CDCl_3$, 100 MHz) δ 12.8 (CH_3), 22.5 (CH_2), 117.3, 120.2, 120.3, 120.6, 123.0, 123.7, 124.3, 127.0, 127.2, 128.0, 128.1, 128.2, 128.8, 130.7, 130.9, 132.0, 140.0, 141.4, 142.0, 143.1, 144.0, 146.1, 148.7, 149.4, 149.9, 152.6, 168.5; EIMS (m/z, I_{rel} %): 589 $[M + 1]^+$ (47), 588 $[M]^+$ (100), 294 (31); Exact mass for $C_{42}H_{28}N_4$ (588.2314). Calcd: C, 85.69; H, 4.79; N, 9.52 %. Found: C, 85.62, H, 4.89, N, 9.63%.

5. Conclusions

A series of novel donor–acceptor fluorophores based on 2-aryl[1,2,4]triazolo[1,5-*c*]quinazolines were successfully synthesized via Suzuki–Miyaura cross-coupling of 5-chloro-substituted precursors with various arylboronic acids. The introduction of electron-donating arylamino groups at the 5-position resulted in strongly emissive compounds in non-polar media such as toluene, with emission profiles sensitive to the nature of the substituents and the degree of π-conjugation. Additional derivatives bearing a phenylene π-spacer were synthesized to modulate donor–acceptor interactions and evaluate the influence of spatial separation on photophysical behaviour. The synthesized compounds were systematically investigated in solvents of varying polarity and in the solid state. Several representatives exhibited pronounced positive solvatochromism, consistent with an intramolecular charge transfer (ICT) excited state. Moreover, the response to acid stimuli was evaluated using trifluoroacetic acid as a protonating agent. The observed acidochromic shifts and fluorescence quenching patterns were found to be structure-dependent and were rationalized based on conjugation effects and protonation site preferences. These experimental findings were further supported by DFT calculations of the frontier molecular orbitals and electronic transitions. The computed HOMO–LUMO energies and electron density distributions provided insight into the nature of the ICT process and explained the differing sites of protonation observed among the derivatives.

Overall, the triazoloquinazoline-based fluorophores described herein demonstrate tunable photophysical properties, environmental sensitivity, and structural versatility, making them promising candidates for applications in fluorescent sensing, stimuli-responsive materials, and organic optoelectronic devices.

Supplementary Materials: The following supporting information can be downloaded at: www.mdpi.com/xxx/s1, Figures S1–S10: NMR and mass spectra of intermediates; Figure S11: molecular structure of **6**, **10**, **11** and atoms numbering; Figures S12–S25: NMR and mass spectra of target products 6a-j, 10,

© 2025 by the author(s). Distributed under a Creative Commons CC BY license.

Preprints.org (www.preprints.org) | NOT PEER-REVIEWED | Posted: 22 October 2025 doi:10.20944/preprints202510.1579.v1

11 and 12a,b; Tables S1–S8: Selected bond lengths and angles of compounds **6g**, **10**, and **12a**; Figure S26: Absorption and emission spectra of compounds **6a-j, 10, 11** and **12a,b** in toluene and MeCN; Figure S27: Changes in emission color of compounds **6a-c**, **10** and **11** in different solvents; Figure S28. Combined emission spectra (non-normalized and normalized) of compounds **6a**, **6b**, **6c** and **10** in different solvents; Tables S9–S11: Empirical solvent polarity parameter (E^{N}_{T}), absorption and emission maxima (λ_{abs}, λ_{em}, nm) and Stokes shift (nm, cm^{-1}) of **6b**, **6c** and **10** in different solvents; Figure S29: Plots of Stokes shift of compounds **6b**, **6c** and **10** versus Reichardt solvent polarity functions; Figure S30: Emission color changes of compounds **6a** and **10** in toluene upon successive addition of trifluoroacetic acid (TFA) and triethylamine (TEA). **Figure S31-S32.** Absorption and emission spectra changes of **6a** and **10** in toluene upon addition of CF_3COOH (TFA)**;** Table S123: The electronic distribution in HOMO/LUMO of **6a-c,e,h,j**, **10**, **11** and **12a,b** for gas phase; Table S13: The optimized geometries of **6a-c,e,h,j**, **10**, **11** and **12a,b** in toluene and MeCN; Table S14: Selected dihedral angles (α), and bond lengths (L) in the optimized geometries of compounds **6a-c,e,h,j, 10, 11** and **12a,b**, in ground (S_0) and excited (S_1) states.

Author Contributions: Conceptualization, E.V.N.; methodology, A.E.K., Y.V.P., and T.N.M.; investigation, A.E.K., E.S.S., and P.A.S.; theoretical calculations, A.S.N.; writing—original draft preparation, T.N.M. and E.V.N.; supervision and project administration, E.V.N. All authors have read and agreed to the published version of the manuscript.

Funding: The research funding from the Ministry of Science and Higher Education of the Russian Federation (Ural Federal University Program of Development within the Priority-2030 Program) is gratefully acknowledged.

Institutional Review Board Statement: Not applicable.

Informed Consent Statement: Not applicable.

Data Availability Statement: The data are available on request from the corresponding authors.

Acknowledgments: The quantum chemical calculations were supported by the RUDN University Scientific Projects Grant System, project № 021342-2-000. Spectral data were obtained in the Laboratory of Complex Research and Expert Evaluation of Organic Materials, Center for Collective Use of unique equipment of the Ural Federal University, https://ckp.urfu.ru.

Conflicts of Interest: The authors declare no conflicts of interest.

References

1. Nosova, E.V.; Lipunova, G.N.; Permyakova, Y.V.; Charushin, V.N. Quinazolines annelated at the N(3)–C(4) bond: Synthesis and biological activity. *Eur. J. Med. Chem.* **2024**, *271*, 116411, doi:10.1016/j.ejmech.2024.116411.
2. Abuelizz, H.A.; Al-Salahi, R. An overview of triazoloquinazolines: Pharmacological significance and recent developments. *Bioorg. Chem.* **2021**, *115*, 105263, doi:10.1016/j.bioorg.2021.105263.
3. Nosova, E.V.; Lipunova, G.N.; Permyakova, J.V.; Charushin, V.N. Chemosensors based on quinazoline moieties. *Dye. Pigment.* **2025**, *235*, 112638, doi:10.1016/j.dyepig.2025.112638.
4. Oh, H.-S.; Lee, H.-J.; No Y.-S.; Eum S.-J.; Lee J.-D.; Kim K.-Y. Preparation of nitrogen-containing polycyclic compounds as organic light-emitting device materials. Patent WO2015008908. 2015.
5. Sun, E.; Fang, R.; Liu, S.; Wu, J. Compound and Application Thereof. Patent CN113527302A. 2021.
6. Achelle, S.; Rodríguez-López, J.; Guen, F.R. Photoluminescence Properties of Aryl-, Arylvinyl-, and Arylethynylpyrimidine Derivatives. *ChemistrySelect* **2018**, *3*, 1852–1886, doi:10.1002/slct.201702472.
7. Kopotilova, A.E.; Moshkina, T.N.; Nosova, E.V.; Lipunova, G.N.; Starnovskaya, E.S.; Kopchuk, D.S.; Kim, G.A.; Gaviko, V.S.; Slepukhin, P.A.; Charushin, V.N. 3-Aryl-5-aminobiphenyl Substituted [1,2,4]triazolo[4,3-c]quinazolines: Synthesis and Photophysical Properties. *Molecules* **2023**, *28*, 1937, doi:10.3390/molecules28041937.
8. Nosova, E.V.; Kopotilova, A.E.; Ivan'kina, M.A.; Moshkina, T.N.; Kopchuk, D.S. Synthesis of 5-(4-bromophenyl)- and 5-(5-bromothiophen-2-yl)-substituted 3-aryl[1,2,4]triazolo[4,3-c]quinazolines. *Russ. Chem. Bull.* **2022**, *71*, 1483–1487, doi:10.1007/s11172-022-3554-7.
9. Moshkina, T.N.; Kopotilova, A.E.; Ivan'kina, M.A.; Starnovskaya, E.S.; Gazizov, D.A.; Nosova, E.V.; Kopchuk, D.S.; El'tsov, O.S.; Slepukhin, P.A.; Charushin, V.N. Design, Synthesis, and Photophysical

© 2025 by the author(s). Distributed under a Creative Commons CC BY license.

Preprints.org (www.preprints.org) | NOT PEER-REVIEWED | Posted: 22 October 2025 doi:10.20944/preprints202510.1579.v1

Properties of 5-Aminobiphenyl Substituted [1,2,4]Triazolo[4,3-c]- and [1,2,4]Triazolo[1,5-c]quinazolines. *Molecules* **2024**, *29*, 2497, doi:10.3390/molecules29112497.

10. Sun, E.; Fang, R.; Liu, S. Organic Compound for Light-Emitting Device, Application of Organic Compound and Organic Light-Emitting Device. Patent CN112174968A 2021.
11. Lefranc, J.; Schmecs, N.; Zorn, L.; Meier, R.; Herbert, S.; Günther, J.; Gutcher, I.; Röse, L.; Bader, B.; Stöckigt, D.; Gorjánácz, M.; Kober, C.; Buchmann, B.; Böhme, S.; Bothe, U.; Platten, M.; Baumann, D. [1,2,4]Triazolo[1,5-*c*]quinazolin-5-amines, Patent WO2021/028382. 2021.
12. Burbiel, J.C.; Ghattas, W.; Küppers, P.; Köse, M.; Lacher, S.; Herzner, A.; Kombu, R.S.; Akkinepally, R.R.; Hockemeyer, J.; Müller, C.E. 2-Amino[1,2,4]triazolo[1,5-*c*]quinazolines and Derived Novel Heterocycles: Syntheses and Structure–Activity Relationships of Potent Adenosine Receptor Antagonists. *ChemMedChem* **2016**, *11*, 2272–2286, doi:10.1002/cmdc.201600255.
13. Balo, C.; López, C.; Brea, J.M.; Fernánde, F.; Caamaño, O. Synthesis and Evaluation of Adenosine Antagonist Activity of a Series of [1,2,4]Triazolo[1,5-c]quinazolines. *Chem. Pharm. Bull.* **2007**, *55*, 372–375, doi:10.1248/cpb.55.372.
14. El-Serwy, W.S.; Mohamed, A.N; Kassem, M.M.E; Mahmoud, K.M.M. Synthesis, Biological Evaluation and Docking Analysis of Some Novel Quinazolin Derivatives as Antitumor Agents. *Iran J Pharm Res.* **2016**, *15*, 179–196.
15. Bilyi, A.K.; Antypenko, L.M.; Ivchuk, V.V.; Kamyshnyi, O.M.; Polishchuk, N.M.; Kovalenko, S.I. 2-Heteroaryl-[1,2,4]triazolo[1,5-*c*]quinazoline-5(6*H*)-thiones and Their S-Substituted Derivatives: Synthesis, Spectroscopic Data, and Biological Activity. *Chempluschem* **2015**, *80*, 980–989, doi:10.1002/cplu.201500051.
16. Wesseler, F.; Lohmann, S.; Riege, D.; Halver, J.; Roth, A.; Pichlo, C.; Weber, S.; Takamiya, M.; Müller, E.; Ketzel, J.; и др. Phenotypic Discovery of Triazolo[1,5-*c*]quinazolines as a First-In-Class Bone Morphogenetic Protein Amplifier Chemotype. *J. Med. Chem.* **2022**, *65*, 15263–15281, doi:10.1021/acs.jmedchem.2c01199.
17. Bader, B.; Zorn, L.; Bothe, U.; Günther, J.; Platten, M.; Röse, L.; Kober, C.; Lefranc, J.; Schmees, N.; Meier, R.M.; Herbert, S.A.; Gutcher, I.; Stöckigt, D.; Gorjánácz, M.; Buchmann, B.; Böhme, S.; Baumann, D. [1,2,4]Triazolo[1,5-*c*]quinazolin-5-amines. Patent CO2022001257. 2022.
18. Porrès, L.; Holland, A.; Pålsson, L.O.; Monkman, A.P.; Kemp, C.; Beeby, A. Absolute measurements of photoluminescence quantum yields of solutions using an integrating sphere. *J. Fluoresc.* **2006**, *16*, 267–273, doi:10.1007/s10895-005-0054-8.
19. Gao, Y.; Zhang, S.; Pan, Y.; Yao, L.; Liu, H.; Guo, Y.; Gu, Q.; Yang, B.; Ma, Y. Hybridization and de-hybridization between the locally-excited (LE) state and the charge-transfer (CT) state: a combined experimental and theoretical study. *Phys. Chem. Chem. Phys.* **2016**, *18*, 24176–24184, doi:10.1039/C6CP02778D.
20. Ravi, M.; Soujanya, T.; Samanta, A.; Radhakrishnan, T.P. Excited-state dipole moments of some Coumarin dyes from a solvatochromic method using the solvent polarity parameter, E. *J. Chem. Soc. Faraday Trans.* **1995**, *91*, 2739–2742, doi:10.1039/FT9959102739.
21. Reichardt, C. Solvatochromic dyes as solvent polarity indicators. *Chem. Rev.* **1994**, *94*, 2319–2358.
22. Lippert, V.E. Spektroskopische Bestimmung des Dipolmomentes aromatischer Verbindungen im ersten angeregten Singulettzustand. **1957**, *853*, 962–975.
23. Mataga, N.; Kaifu, Y.; Koizumi, M. Solvent Effects upon Fluorescence Spectra and the Dipolemoments of Excited Molecules. *Bull. Chem. Soc. Jpn.* **1956**, *29*, 465–470, doi:10.1246/bcsj.29.465.
24. Bakhshiev, N.G. Universal intermolecular interactions and their effect on the position of the electronic spectra of molecules in two component solutions. *Opt. Spektrosk.* **1964**, *16*, 821–832.
25. Suppan, P. Excited-state dipole moments from absorption/fluorescence solvatochromic ratios. *Chem. Phys. Lett.* **1983**, *94*, 272–275, doi:10.1016/0009-2614(83)87086-9.
26. Bonnaud, T.; Scaviner, M.; Robin-le Guen, F.; Achelle, S. 4-substituted push-pull quinazoline chromophores with extended π-conjugated linker. *J. Heterocycl. Chem.* **2024**, *61*, 358–364, doi:10.1002/jhet.4768.
27. Nosova, E.V.; Moshkina, T.N.; Lipunova, G.N.; Kopchuk, D.S.; Slepukhin, P.A.; Baklanova, I. V.; Charushin, V.N. Synthesis and Photophysical Studies of 2-(Thiophen-2-yl)-4-(morpholin-4-yl)quinazoline Derivatives. *European J. Org. Chem.* **2016**, *2016*, 2876–2881, doi:10.1002/ejoc.201600404.

© 2025 by the author(s). Distributed under a Creative Commons CC BY license.

Preprints.org (www.preprints.org) | NOT PEER-REVIEWED | Posted: 22 October 2025 doi:10.20944/preprints202510.1579.v1

28. Dolomanov, O.V.; Bourhis, L.J.; Gildea, R.J.; Howard, J.A.K.; Puschmann, H. OLEX2: A complete structure solution, refinement and analysis program. *J. Appl. Crystallogr.* **2009**, *42*, 339–341, doi:10.1107/S0021889808042726.
29. Sheldrick, G.M. SHELXT – Integrated space-group and crystal-structure determination. *Acta Crystallogr. Sect. A Found. Adv.* **2015**, *71*, 3–8, doi:10.1107/S2053273314026370.
30. Frisch, M.J.; Trucks, G.W.; Schlegel, H.B.; Scuseria, G.E.; Robb, M.A.; Cheeseman, J.R.; Scalmani, G.; Barone, V.; Petersson, G.A.; Nakatsuji, H.; Li, X.; Caricato, M.; Marenich, A.V.; Bloino, J.; Janesko, B.G.; Gomperts, R.; Mennucci, B.; Hratchian, H. P.; Ortiz, J.V.; Izmaylov, A.F.; Williams-Young, D.; Ding, F.; Lipparini, F.; Egidi, F.J.; Goings, B.P.; Petrone, A.; Henderson, T.D.R.; Zakrzewski, V.G.; Gao, J.; Rega, N.; Zheng, G.W.L.; Hada, M.; Ehara, M.; Toyota, K.; Fukuda, R.J.H.; Ishida, M.; Nakajima, T.; Honda, Y.; Kitao, O.H.N. Gaussian 09, Revision C.01, **2010**, Gaussian Inc., Wallingford.
31. Marenich, A.V.; Cramer, C.J.; Truhlar, D.G. Universal Solvation Model Based on Solute Electron Density and on a Continuum Model of the Solvent Defined by the Bulk Dielectric Constant and Atomic Surface Tensions. *J. Phys. Chem. B* **2009**, *113*, 6378–6396, doi:10.1021/jp810292n.
32. Francis, J.E.; Cash, W.D.; Barbaz, B.S.; Bernard, P.S.; Lovell, R.A.; Mazzenga, G.C.; Friedmann, R.C.; Hyun, J.L.; Braunwalder, A.F. Synthesis and benzodiazepine binding activity of a series of novel [1,2,4]triazolo[1,5-*c*]quinazolin-5(6*H*)-ones. *J. Med. Chem.* **1991**, *34*, 281–290, doi:10.1021/jm00105a044.:

Disclaimer/Publisher's Note: The statements, opinions and data contained in all publications are solely those of the individual author(s) and contributor(s) and not of MDPI and/or the editor(s). MDPI and/or the editor(s) disclaim responsibility for any injury to people or property resulting from any ideas, methods, instructions or products referred to in the content.

© 2025 by the author(s). Distributed under a Creative Commons CC BY license.